

1 The roles of isolation and interspecific interaction in generating the
2 functional diversity of an insular mammal radiation

3
4
5 Jonathan A. Nations^{*1,2}, Brooks A. Kohli³, Heru Handika², Anang S. Achmadi⁴, Michael J.
6 Polito^{5,6}, Kevin C. Rowe⁷, Jacob A. Esselstyn²

7
8
9 ¹Florida Museum of Natural History, University of Florida, Gainesville, Florida, 32611, United
10 States

11 ²Museum of Natural Science and Department of Biological Sciences, Louisiana State University,
12 Baton Rouge, Louisiana, 70803, United States

13 ³Biological Sciences, Ohio University, Athens, Ohio, 45701, United States

14 ⁴Museum Zoologicum Bogoriense, Research Center for Ecology and Ethnobiology, National
15 Research and Innovation Agency (BRIN), Cibinong, Jawa Barat 16911, Indonesia

16 ⁵Department of Oceanography and Coastal Sciences, Louisiana State University, Baton Rouge,
17 Louisiana, 70803, United States

18 ⁶Department of Ocean Sciences, University of California, Santa Cruz, California, 95064, United
19 States

20 ⁷Sciences Department, Museums Victoria, Melbourne, Victoria 3001, Australia

21
22 *Correspondence to be sent to: Florida Museum of Natural History, University of Florida,
23 Gainesville, Florida, 32611, United States; E-mail: jnations@floridamuseum.ufl.edu

24

25

26

27

28

29

30

31

32

33

34

35

36

37

38

39

40

41

42

43

44

Abstract

45 Communities that occupy similar environments but vary in the richness of closely related species
46 can illuminate how functional variation and species richness interact to fill ecological space in
47 the absence of abiotic filtering, though this has yet to be explored on an oceanic island where the
48 processes of community assembly may differ from continental settings. In discrete montane
49 communities on the island of Sulawesi, local murine rodent (rats and mice) richness ranges from
50 7 to 23 species. We measured 17 morphological, ecological, and isotopic traits, both individually
51 and grouped into 5 multivariate traits in 40 species, to test for the expansion or packing of
52 functional space among nine murine communities. We employed a novel probabilistic approach
53 for integrating intraspecific and community-level trait variance into functional richness. Trait-
54 specific and phylogenetic diversity patterns indicate dynamic community assembly due to
55 variable niche expansion and packing on multiple niche axes. Locomotion and covarying traits
56 such as tail length emerged as a fundamental axis of ecological variation, expanding functional
57 space and enabling the niche packing of other traits such as diet and body size. Though trait
58 divergence often explains functional diversity in island communities, we found that phylogenetic
59 diversity facilitates functional space expansion in some conserved traits such as cranial shape,
60 while more labile traits are overdispersed both within and between island clades, suggesting a
61 role of niche complementarity. Our results evoke interspecific interactions, differences in trait
62 lability, and the independent evolutionary trajectories of each of Sulawesi's 6 murine clades as
63 central to generating the exceptional functional diversity and species richness in this exceptional,
64 insular radiation.

65

66

67 Keywords: Community Niche Space, Functional Morphology, Stable Isotopes, Murinae,

68 Bayesian, Sulawesi, Indonesia

69

Introduction

70

71 Whether at a local, continental, or global scale, species richness is not evenly distributed across
72 the landscape. This unevenness emerges from both environmental and resource heterogeneity
73 among communities, and from the interactions among the species within local communities.

74 Local species richness is often positively correlated with the complexity of habitat structure and
75 diversity of available resources (Tews et al. 2004). The observation that different localities with
76 similar habitat structure, resource availability, and historical access often contain ecologically
77 similar communities led to the prediction that species only co-occur if they partition niche space
78 along some axis (herein we consider the niche to be the size and shape of multivariate ecological
79 space that a species utilizes), otherwise one will be excluded through competition (Hutchinson
80 1957, MacArthur & Levins 1967, May & MacArthur 1972, Brown & Lieberman 1973, Brown
81 1975, Pianka 1974, M'Closkey 1978). Competitive exclusion can be mitigated if two co-
82 occurring species use a narrower breadth of resources, producing a more densely packed
83 community niche space ("niche packing"), or if they exploit habitats or resources that are unused
84 or non-existent in low-resource or species-poor communities, leading to a larger community
85 niche space ("niche expansion"; MacArthur 1965, 1970, Pigot et al. 2016, Oliveira et al. 2020).

86 The foundational work on competition's role in community assembly relied on empirical data
87 from continental communities with equal biogeographic accessibility but variation in primary
88 productivity or habitat complexity (Brown & Lieberman 1973, Brown 1975, M'Closkey 1978,
89 Karr & James 1975, Pianka 1974, Weiher & Keddy 1995), or from archipelagos where island
90 size or geographic complexity determines resource availability and habitat area, both of which
91 influence overall species richness (Wilson 1961, Diamond 1975, Lister 1976, Gillespie 2004,

92 Losos 2009, Losos & Ricklefs 2009). Less explored are insular areas of similar habitat structure
93 and resource availability, but with discrete communities that vary in species richness (“species
94 richness anomalies”, Swenson et al. 2016 pg. E83). Yet, these anomalies offer powerful systems
95 for interrogating the role of competition in the distribution of functional diversity within and
96 among communities because the effects of abiotic processes such as habitat filtering are
97 minimized (Swenson et al 2016, Li et al. 2017). Most studies of species richness anomalies have
98 examined plants in continental settings (Latham & Ricklefs 1993, Swenson et al. 2016, Xu et al.
99 2019) where environmental and historical processes influence the regional species pool. Few, if
100 any, studies have tested the role of competition in the assembly of discrete communities nested
101 within an insular setting where species pools are formed through long-distance colonization and
102 in-situ diversification.

103

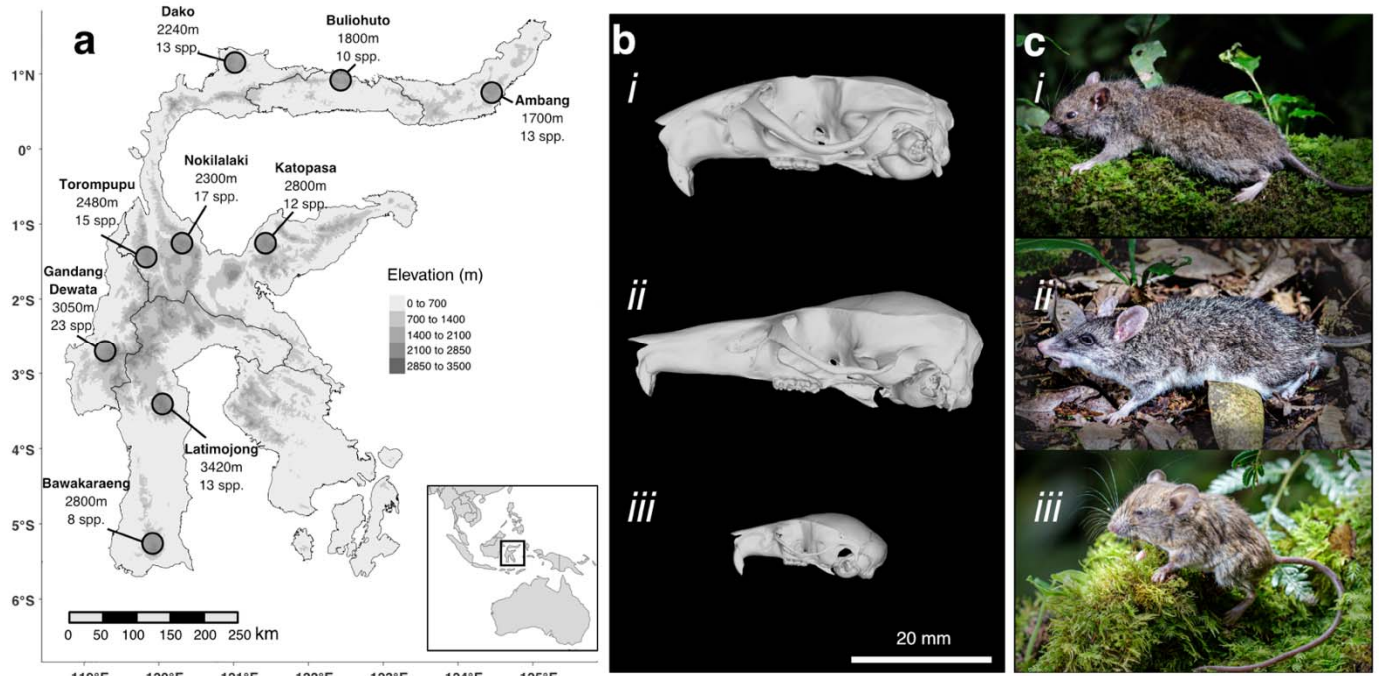
104 Oceanic islands are often hotspots of diversification and endemism, and their unique
105 biogeographic and historical conditions can help illuminate the ecological and evolutionary
106 processes that structure local communities (Losos & Ricklefs 2009). Lineages that arrive and
107 diversify in isolated locations regularly undergo ecological shifts that result in behaviors or
108 phenotypes that are uncommon or non-existent in source communities (Carlquist 1966, Millen
109 2006, Pinto et al. 2008, Esselstyn et al. 2012, 2015, 2021, Stroud & Losos 2016). The presence
110 of high functional and ecological disparity within an endemic radiation may affect community
111 structure in multiple ways. First, there is some evidence that community assembly occurs
112 differently on continents and islands. Using an assortment of phenotypic and behavioral proxies
113 for resource use across a variety of spatial scales, niche packing is frequently invoked as the
114 primary process of assembly in species-rich animal communities on continents (Brown 1975,

115 Karr & James 1975, M'Closkey 1978, MacArthur & MacArthur 1961, Pianka 1974, Pigot et al.
116 2016, Van de Perre et al. 2020). However, niche expansion has found some support among
117 isolated island communities of many closely related species (Lister 1976). Second, multiple
118 lineages evolving in sympatry within an insular setting often promotes niche divergence through
119 adaptive diversification, reducing phylogenetic niche conservatism (Losos et al. 2003). As a
120 result, the niche breadth of a community within an insular setting, despite the lower phylogenetic
121 diversity, may equal that of a similar continental community. Importantly, quantifying trait
122 differences following adaptive diversification among closely related species can illuminate
123 which traits are most evolutionary labile and/or important for resource partitioning (Losos et al.
124 2003, Hiller et al. 2019, Dorey et al. 2020, Stroud 2021).

125

126 The murine rodent fauna (rats and mice in the subfamily Murinae) of Sulawesi,
127 Indonesia, a mountainous, wet tropical, oceanic island at the center of the Wallacean biodiversity
128 hotspot (Figure 1), is an intriguing system for testing patterns of community niche occupancy.
129 First, the murine diversity of Sulawesi is exceptional, with at least 48 endemic species stemming
130 from seven colonist ancestors that arrived from circa 6 Ma to < 1 Ma (Figure S1, Rowe et al.
131 2019, Handika et al. 2021). While some colonists spawned small radiations of species, others are
132 evidenced by only a single living species (Table 1, Figure S1). Each clade is widespread on
133 Sulawesi and most contribute to species richness of all local murine communities on the island.
134 Second, Sulawesi contains some of the most unusual rodent forms found anywhere (Figure 1b,
135 Esselstyn et al. 2012, 2015, Rowe et al. 2014) living in sympatry with more typical “rat-like”
136 morphologies and ecologies. Sulawesi murines have an array of cranial shapes that reflect their
137 dietary preferences (Figure 1b; Esselstyn et al. 2012, 2015, Martinez et al. 2018), consume a

138 broad range of foods such as fruit, seeds, fungi, leaves, roots, and earthworms (Musser 2014,
139 Rowe et al. 2016a), have body sizes ranging from 10 to 500g, and occupy a variety of locomotor
140 modes (arboreal; scansorial; terrestrial; amphibious, Nations et al. 2021). Third, due to the
141 topographic complexity of Sulawesi and the positive correlation between elevation and small
142 mammal diversity in this region (Heaney 2001, Esselstyn et al. 2021), the murine communities
143 on the islands are partitioned into discrete, montane assemblages (Figure 1). The local montane
144 murine communities, defined as the species living on a mountain from the upper-lowland forest
145 to the peak, range from 7 to 23 species, with the upper limit being, to our knowledge, the most
146 diverse local community of closely related terrestrial mammals on Earth. Lastly, the variation in
147 local community richness does not appear to be determined by environmental or habitat
148 differences among mountains but is likely the result of the colonization process outward from the
149 central core to the peninsulas during the island's formation (Hall 2013, Nugraha & Hall 2018,
150 Handika et al. 2021). Maximum elevation, which may correlate with the area occupied by
151 different habitats, appears to play only a minor role in species richness (Figure 1a), and net
152 primary productivity is nearly constant across the island's montane regions (Imhoff et al. 2004),
153 suggesting that environmental filtering, often a central process of community assembly (Webb et
154 al. 2002, Cavender-Bares et al. 2004, Li et al. 2017), does not greatly affect the functional
155 diversity of Sulawesi's murine communities. Together, these properties generate a fascinating
156 hierarchical organization: a species pool of small mammals with disparate ecologies and
157 morphologies living in discrete montane communities that, due to their habitat similarity and
158 striking disparity in richness, represent species-richness anomalies, all of which lie within a
159 remote, oceanic island. Such a system presents a compelling natural experiment for testing
160 alternative hypotheses of how communities assemble to occupy ecological niche space



161

162 **Figure 1:** Small mammal surveys of nine mountains a) on the oceanic island of Sulawesi revealed varying murine
163 rodent species richness across the island. Each mountain on the map is labeled with the maximum elevation and the
164 number of murine rodent species present. All but Latimojong were surveyed within 600m of the summit. b) The
165 diversity of Sulawesi murines is exceptional and includes unique forms that live alongside species with more
166 “typical” ecologies and morphologies, as demonstrated from surfaces of cranial μCT scans of *i* – *Rattus hoffmanni*, a
167 “typical” murine morphology and ecology, *ii* – the shrew rat *Echinothrix leucura* with its extremely elongate rostrum
168 and soft invertebrate diet, *iii* – the arboreal *Haeromys minahassae*, with a short rostrum and very small size. c)
169 Photographs: *i* – *Rattus hoffmanni*, *ii* – *Echinothrix leucura*, and *iii* – *Haeromys minahassae*.

170

171 Here, we test whether increased species richness in environmentally similar communities
172 of montane rodents leads to the expansion or packing of ecological niche space. Observational
173 data, including behavior, life history, and movement patterns, are scarce for the nocturnal,
174 secretive Sulawesi murines. Much of what we know about these species comes from museum
175 specimens and their associated metadata (e.g., locality and habitat details, forest strata
176 preferences, and morphological measurements). Therefore, to infer the ecological niche breadth
177 of each montane assemblage, we quantify diet, trophic dimension, and microhabitat using 12
178 individual functional and ecological traits and five multivariate trait complexes to estimate both
179 the volume and density of community functional space, which we define as the sum of the n-

180 dimensional functional spaces of the species therein. Importantly, individual traits or groups of
181 traits related to the same niche axis can reveal distinct, interacting processes (Spasojevic &
182 Suding 2012, Pigot et al. 2016, Kohli et al. 2021). Additionally, we examine the role of
183 phylogenetic niche conservatism and trait lability in the assembly of these nine montane
184 communities by testing for the influence of phylogenetic diversity and inter-clade variation on
185 functional space occupancy.

186

187

188 **Materials and Methods**

189

190 *The distribution of species-* We compiled occurrence records from nine small mammal
191 inventories of mountain regions on Sulawesi, Indonesia, including one well-documented
192 mountain surveyed from 1973 to 1976 by Guy Musser and colleagues (Mt. Nokilalaki; Musser,
193 2014) and eight mountains surveyed between 2011 and 2016 (Ambang, Bawakaraeng,
194 Buliohuto, Dako, Gandang Dewata, Katopasa, Latimojong, and Torompupu; Figure 1a).

195

196 All surveys began in lower primary forest near the line of anthropogenic forest clearing (1100m
197 to 1500m) and extended to upper-montane forests. All surveys extended to within 600m
198 elevation of the summit except for Latimojong (highest survey site at 2535m, summit at 3400m).
199 Trapping records show that there are no Sulawesi murines restricted to elevations above 2500m,
200 or to habitats within 600m of the summit (Musser 2014). Historical surveys by Musser lasted
201 several months and were conducted over four years, employing a mix of snap traps and live
202 traps. Modern surveys (2011-16) lasted an average of 17 days (11-25) and employed similar

203 collection methods, including a mix of snap traps, live traps, and 20-30L pitfall buckets. All the
204 murine rodent species known from the sampled localities (Musser 2014, Wilson et al. 2019) were
205 collected during these modern surveys, indicating a thorough sampling effort. Five new taxa that
206 were discovered during these expeditions have been described (Musser 2014, Esselstyn et al.
207 2012, Rowe et al. 2014, Esselstyn et al. 2015, Rowe et al. 2016b) and several new locality
208 records resulted (Achmadi, et al., 2014; Handika, et al., 2021). Specimens from all surveys were
209 deposited in the Museum Zoologicum Bogoriense (MZB), Bogor, Indonesia; the American
210 Museum of Natural History (AMNH), New York, USA; Museums Victoria (MV), Melbourne,
211 Australia; the Museum of Vertebrate Zoology (MVZ), Berkeley, USA; the Field Museum of
212 Natural History (FMNH), Chicago, USA; and the Louisiana State University Museum of Natural
213 Science (LSUMZ), Baton Rouge, USA.

214

Clade	Crown Age	Species Sampled
Echinothrix	5.11 (4.49-5.69)	10 (10)
Maxomys	3.72 (3.21-4.29)	5 (5)
Bunomys	3.45 (3.09-3.81)	15 (15)
Margaretamys	2.92 (2.29-3.51)	2 (4)
Rattus*	1.57 (1.22-1.95)	6 (6)
Haeromys [†]	Indeterminate	1 (1)

215 **Table 1:** Ages of six clades descended from Sulawesi colonists. Median age in millions of years is reported with
216 95% credible intervals in parentheses. Species sampled reports the number of species in this study with overall clade
217 richness in parentheses and demonstrates near complete sampling. The two unsampled *Margaretamys* species were
218 not detected in the localities in this study. All ages taken from Rowe et al. 2019. *There were likely two
219 colonizations by the ancestors of native *Rattus* spp., the second of which occurred 1.16-0.6 Ma (Rowe et al. 2019),
220 however, all *Rattus* in this study form a clade relative to other Sulawesi murines. Two human commensal *Rattus*
221 spp. found on Sulawesi were excluded. [†]The age of arrival of the Haeromys clade is unknown as other species of
222 Haeromys from Borneo have yet to be included in phylogenetic analyses.
223

224 *Functional trait data collection and processing-* We compiled or generated functional trait
225 values for 11 continuous traits and one discrete trait for all available Sulawesi murines from each
226 of the nine communities. Individual Sulawesi murine species exhibit little intraspecific
227 morphological variation among localities, far less than the morphological differences among

228 species (Musser 2014), and we therefore combined measurements of individual species from
229 multiple localities and estimated trait distributions using probabilistic methods to overcome the
230 limited availability of some traits. Detailed information on traits, sample sizes, data processing,
231 and multivariate trait composition are available in Table S1. All data, models, and output files
232 are available in Dryad Repository (to be added prior to publication).

233

234 *Morphological data collection*- We assembled external measurement data from 630 specimens,
235 including head-body length (mm), tail length (mm), hind-foot length (mm), ear length (mm), and
236 mass (g), from previously published sources (Wilson et al. 2019, Nations et al. 2021) and online
237 museum databases. Measured specimens were from the nine surveyed mountains and other
238 localities on Sulawesi. To obtain ecologically relevant features of external measurements and
239 mitigate the influence of size in some of our analyses, we calculated three commonly used ratios:
240 Relative tail length (tail length / (head-body length + tail length)), relative hind-foot length (hind-
241 foot length / head-body length), and relative ear length (ear length / head-body length) (Nations
242 et al. 2021, Table S1).

243

244 The shape of a rodent's skull and lower jaw provides a wealth of indirect ecological
245 information on foraging, feeding, and sensory processing, and is often used as a proxy for
246 fundamental dietary niche (Samuels 2009). We generated μ CT scans of the cranium of 64
247 specimens from 38 species and the mandible of 61 specimens from 36 species (Table S1). Scans
248 were generated from specimens collected in the nine surveys, as well as from previously
249 collected museum materials. Stacks of 2D Tiff files were imported to MorphoDig, where 3D
250 landmarks were placed on cropped volume renderings (Lebrun, 2018). We placed 67 cranial

251 landmarks (Figure S2) on the left side of the skull, unless damage caused us to use the right side,
252 in which case we reversed the rendering on the Z-axis. In separate renderings, we placed 20
253 landmarks on the left dentary of the mandible (Figure S2). Landmarks were exported from
254 MorphoDig as .stv files and imported into the R package geomorph v.4.0.3 for processing
255 (Adams et al. 2021, Baken et al. 2021). Missing landmarks (11 of 4288 cranial and three of 1220
256 mandible landmarks) were imputed, a generalized Procrustes analysis (GPA) superimposition
257 was performed, and shape coordinates were subjected to a principal components analysis. We
258 retained the centroid size (an estimate of total size) and the scores from the first 36 principal
259 components of the cranium and 20 axes of the mandible, each representing >95% of the shape
260 variation of the element.

261

262 *Stable isotope data collection-* Approximately 1-2 grams of hairs were plucked from the rump of
263 286 dry museum specimens collected on six focal surveys (Ambang, Bawakaraeng, Buliohuto,
264 Dako, Gandang Dewata, and Latimojong). Isotopic values can vary regionally (Fry 2006);
265 therefore, we collected hair samples from multiple individuals of each species from each locality
266 (mean = 4.6 specimens/species/locality, range = 1-14). Nitrogen stable isotope values ($\delta^{15}\text{N}$) act
267 as a proxy for consumer trophic position as they generally increase by 3–5% per trophic level
268 (DeNiro & Epstein 1981). Carbon isotope values ($\delta^{13}\text{C}$) generally exhibit little to no change with
269 trophic position and are commonly used as proxies of consumer's basal carbon resource use (e.g.
270 use of differing primary production energy pathways; DeNiro & Epstein 1978). Combined, these
271 two metrics are commonly used to quantify the “isotopic niche” of consumers, which can act as a
272 useful proxy of species realized dietary niche (Newsome et al. 2007, Ben-David & Flaherty
273 2012). Stable isotope values are reported in delta notation in per mil units. Samples were

274 processed at the Stable Isotope Ecology Laboratory, Department of Oceanography & Coastal
275 Sciences, Louisiana State University. Details on sample cleaning, processing, and analysis are in
276 the Supporting Methods.

277

278 *Locomotor mode data collection*- We used the locomotor classification scheme from Nations et
279 al. (2019, 2021) to group each Sulawesi murine into one of four discrete locomotor modes:
280 Arboreal, (climbing is integral to survival); General (navigates a variety of substrates and habitat
281 strata); Terrestrial (on the ground surface); and Amphibious, (dependent on aquatic habitats for
282 foraging).

283

284 *Combined traits* – We combined our 11 continuous traits into five multivariate traits that
285 represent distinct niche dimensions: (1) head shape (cranium shape PC 1-36 and mandible shape
286 PC 1-20); (2) isotopic niche space ($\delta^{15}\text{N}$ and $\delta^{13}\text{C}$ stable isotope values); (3) body proportions
287 (head-body length, relative tail length, relative hind-foot length, and relative ear length); (4) body
288 size (log(mass) and head-body length); and (5) total morphological shape (all nine morphological
289 traits). We did this by combining the predicted trait values for each community (see below).

290

291 *Estimating species' trait values*- The sample size of morphological and isotopic data varied
292 between species and mountain communities, and in some cases was limited to one individual,
293 such as with the amphibious *Waiomys mammasae*, a species known from a single specimen
294 (Rowe et al. 2014). To mitigate uneven sampling, we estimated a probability distribution of
295 species trait values using partial-pooling in a multilevel Bayesian model. Unlike complete
296 pooling (one global mean estimated for all combined samples) or no-pooling (one mean

297 estimated per species, independent of all others), partial-pooling estimates a mean for each
298 species as well as the variance among species, which serves as an adaptive prior that is common
299 to all the species' means (McElreath 2020). The Bayesian partial-pooling modeling allowed us to
300 incorporate intraspecific variation in trait value predictions while avoiding point estimates such
301 as averages, which discard valuable information. This approach prevents unbalanced estimates
302 by using the trait-variance probability estimates from well-sampled species to inform variance
303 estimates of species with fewer samples (Gelman & Hill 2006, McElreath 2020). All analyses
304 were conducted in the probabilistic programming language Stan (Carpenter et al. 2017) within
305 the R library brms v. 2.17.0 (Bürkner 2018). Subsequent data processing and figuring relied on
306 the R libraries tidyverse v. 1.3.1 (Wickham et al. 2020), furrr v. 0.3.0 (Vaughan 2021), and
307 tidybayes v. 3.0.2 (Kay 2020). All data, scripts, and output files are available in Zenodo
308 Repository (to be added prior to publication) and on GitHub (to be added).

309

310 For each continuous trait (Table S1), we used the trait value as the response variable, and
311 used species as a group-level predictor. All traits were scaled to unity prior to analyses. We used
312 the student-*t* distribution to describe the response variable to minimize the influence of rare,
313 extreme observations (a.k.a. 'robust regression', Kruschke 2013, McElreath 2020). Each model
314 included four chains with 4000 iterations of warm-up and 1000 sampling iterations. Posterior
315 predictions from the four chains were combined, resulting in 4000 samples per trait per species.
316 To mitigate the potential geographic signal in stable isotope values (Fry 2006), and facilitate
317 randomization (see below), the posterior estimates of the $\delta^{15}\text{N}$ and $\delta^{13}\text{C}$ stable isotope values
318 were estimated with models that included an additional 'community' group-level effect, but
319 otherwise were identical to the models described above (Supporting Methods). These stable

320 isotope models generated posterior values of species' isotopic measurements conditioned on the
321 locality, enabling comparisons among communities and randomized sampling for null models
322 (Table S1, Figure S3). Full details of the model, prior, and chain-estimation are described in the
323 Supporting Methods.

324

325 *Estimating functional space volume* – We defined functional space volume as the total volume of
326 n-dimensional trait space occupied by species in a community, and for consistency and clarity
327 we use the term 'functional space volume' for all individual and multivariate traits, regardless of
328 dimension. We used the sum of the variance of each trait value to estimate the volume of
329 community functional space for each community, which is less sensitive to outliers and
330 outperforms other metrics such as ellipse volumes, convex hull volumes, and hypervolumes,
331 especially for functional spaces with many axes (Li et al. 2017, Guillerme et al. 2020). We
332 estimated a posterior distribution of the variance of each trait for each community by first
333 grouping the species' trait value estimates by community. Then, for each of the 4000 posterior
334 draws (one draw ranging between 7 and 23 values, depending on the richness of the community),
335 we estimated the variance of the trait, resulting in a distribution of 4000 variance values for each
336 trait for each community. We estimated the combined multivariate trait space variance by
337 summing the variances of each trait, then dividing by the number of traits. We estimated the 89%
338 probability values for the variance of each individual and combined trait space. To estimate
339 locomotor mode variance, we dummy coded locomotor mode into four binary columns (one per
340 mode) and performed a redundancy analysis (Legendre & Legendre 2012) with the rda()
341 function in the vegan package (Oksanen et al. 2019). We then extracted the PC scores for each
342 species and calculated the sum of variances of the three PC axes for each community.

343

344 *Estimating functional space density*- We estimated the density of species within functional trait
345 space with the mean nearest neighbor (NN) metric (Guillerme et al. 2020). Our methods follow
346 the estimates of functional space volume above. First, we grouped species' trait values by
347 community, then estimated the individual trait density for each posterior draw using the NN
348 metric in the disparity() function of the R library dispRity (Guillerme 2018), resulting in a
349 distribution of 4000 NN values for each trait and combined trait space. To estimate locomotor
350 mode density, performed a redundancy analysis on the dummy-coded locomotor data as above.
351 We then extracted the PC scores for each species, grouped the species by community, and
352 estimated the NN value for each community as with the continuous traits above, in this case
353 generating only a single NN value per community rather than a distribution.

354

355 *Null models of functional space volume and density*- We used null models to determine the
356 difference between the functional space of our nine communities and randomly assembled
357 communities. For each community we created 1000 randomized null communities of $n_{community}$
358 species for each of the nine localities using the independent swap algorithm (Gotelli 2001). We
359 then calculated both volume and density as above for each individual (n=12) and combined
360 (n=5) trait for each of the 1000 randomized community samples. Standardized effect size (SES)
361 was calculated as:

$$362 \quad SES = \frac{Trait_{observed} - Mean(Trait_{Random})}{SD(Trait_{Random})},$$

363 where $Trait_{observed}$ is the vector of 4000 samples of the density or volume of the given trait,
364 $Mean(Trait_{Random})$ and $SD(Trait_{Random})$ are the mean and standard deviation of the density
365 or volume values of the given trait from the 1000 random species assemblies. Positive SES

366 values indicate greater than random functional space volume or lower than random functional
367 space density (overdispersion), meaning that species in that community are occupying functional
368 space outside the range of other communities and/or their niches are farther apart in functional
369 space (niche expansion). Negative SES values indicate lower than random functional space
370 volume and greater than random functional space density (underdispersion or clustering),
371 meaning that species in that community are occupying less ecological space than other
372 communities and/or their niches are closer together in functional space (niche packing; Oliveria
373 et al. 2020).

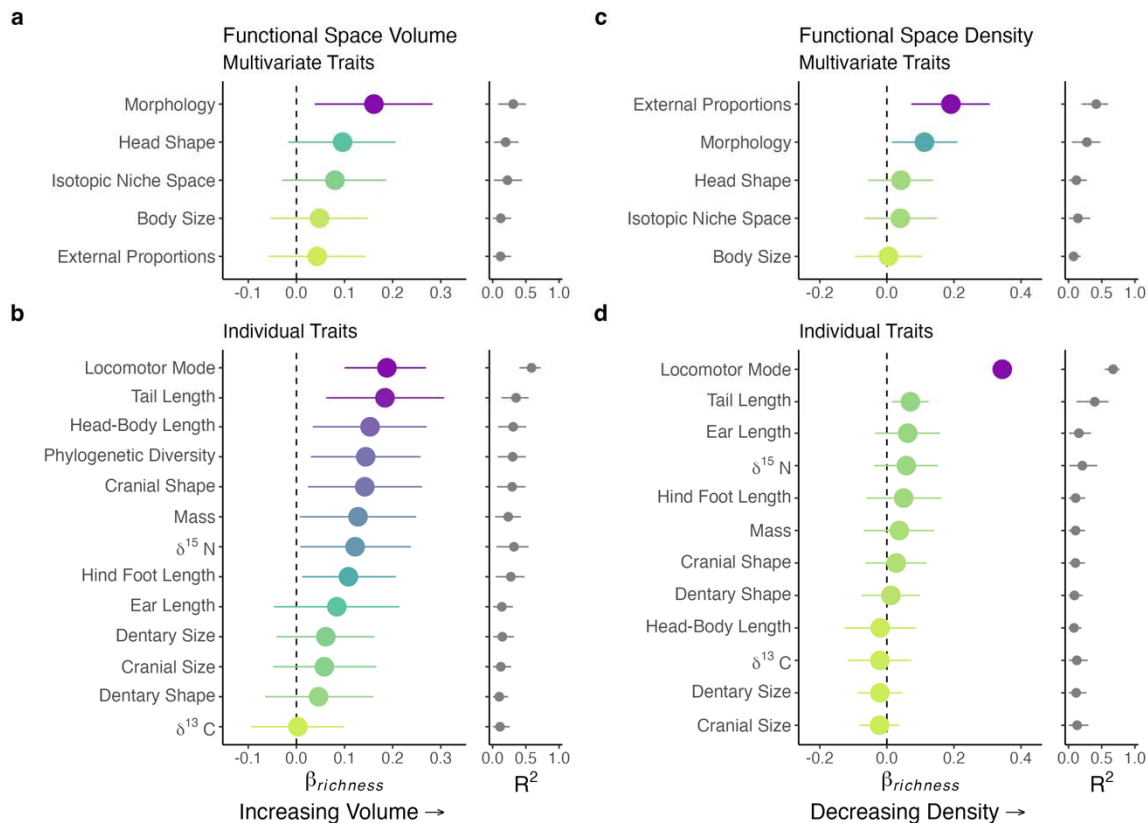
374

375 *Effect of species richness on community functional space volume and density-* If niche expansion
376 is the primary mode of resource partitioning in Sulawesi murine communities, then we expected
377 that functional space volume will increase with increasing species richness, and that functional
378 space density will remain stable as richness increases. Whereas if niche packing is occurring, we
379 expected that functional space density will increase with species richness, and that there will be
380 no effect of richness on functional space volume. To quantify the effect size of richness
381 ($\beta_{richness}$) on functional space volume and density, we used Bayesian linear regression models
382 that include the measurement error of the predictor variable to estimate the effect size of species
383 richness on volume or density. We used species richness as the predictor variable, and the mean
384 and standard error of the trait estimates for each community as the response. Measurement error
385 models contain vastly more information per observation than a single point observation and
386 provide robust estimates despite the small number of sampled communities (Bürkner 2018,
387 McElreath 2020). We also calculated the Bayesian R^2 value for each regression (Gelman et al.
388 2019). The models, priors, and chain estimations are detailed in the Supporting Methods.

389

390 *Phylogenetic diversity as a path to trait disparity*- The ecological space occupied by a
391 community may depend on which lineages or clades are present (Webb 2000). Trait disparity
392 appears to vary among clades of Sulawesi murines, and if so, then the volume and densities of
393 functional spaces may be more influenced by phylogenetic diversity than ecological factors. To
394 determine how phylogenetic diversity mediates functional space occupancy in the nine murine
395 communities, we estimated the phylogenetic diversity (PD) of each community using Faith's
396 metric of branch length (Faith 1996). We removed all but the Sulawesi species ($n = 35$) from a
397 time-calibrated phylogenetic hypothesis of Murinae (Nations et al. 2021). For the analyses
398 described above, we had trait data for four species that are not included in this phylogeny:
399 *Maxomys wattsi*, *Rattus bontanus*, *Rattus mollicomulus*, and *Rattus marmosurus*. We manually
400 added these four species into the tree using the R package phytools (Revell 2012). Details are
401 found in the Supplemental Methods. We used the R package picante (Kembell et al. 2010) to
402 estimated Faith's metric of PD, and to sample 1000 random communities in order to calculate the
403 SES value of PD (SES PD). We used linear modeling in brms to estimate the effect size of
404 species richness on SES PD. *Haeromys minahassae* is the only representative of its genus on
405 Sulawesi, and, due to its large phylogenetic distance from other Sulawesi murines, may have an
406 oversized impact on estimates of community PD. Therefore, we repeated the estimates of SES
407 PD and effect size above without *Haeromys minahassae*. To quantify the trait disparity within
408 and among Sulawesi murine clades, we grouped the posterior distributions of the species'
409 predicted trait values by clade, then estimated the variance of each of the 12 univariate traits. We
410 plotted the trait value variance for each community along with the species' predicted trait values
411 (Figure S4)

412



413

414 **Figure 2:** The effect of species richness on community functional space volume (a, b) and density (c, d). X-axes
415 show the $\beta_{richness}$ estimates (the regression slope) for each trait space (y-axis) on the left and the Bayesian R^2 for
416 each $\beta_{richness}$ estimate on the right. Colored point intervals show 89% probability of $\beta_{richness}$ estimates (effect
417 size), with color varying by $\beta_{richness}$ value. Black point intervals show 50% posterior estimates of Bayesian R^2 for
418 each trait space. Density was estimated using the mean nearest neighbor (NN), and a high NN distance indicates low
419 density. Four of the five multivariate traits (a) and seven of the 12 individual traits (b), show an increase in
420 functional space volume (trait variance) with greater richness (i.e., positive $\beta_{richness}$). Phylogenetic diversity also
421 increases with species richness (b). All multivariate traits (c) and individual traits (d) show a stable or, surprisingly,
422 decreasing functional space density (increased NN distance) with greater species richness.

423

Results

425

426 *Models of trait values-* All parameters in the Bayesian multilevel model estimates of trait-value
427 distributions and measurement-error estimates of the species richness effect on trait values had
428 ESS > 1000 and a Gelman-Rubin diagnostic $\hat{R} \leq 1.01$, indicating convergence. Raw volume and

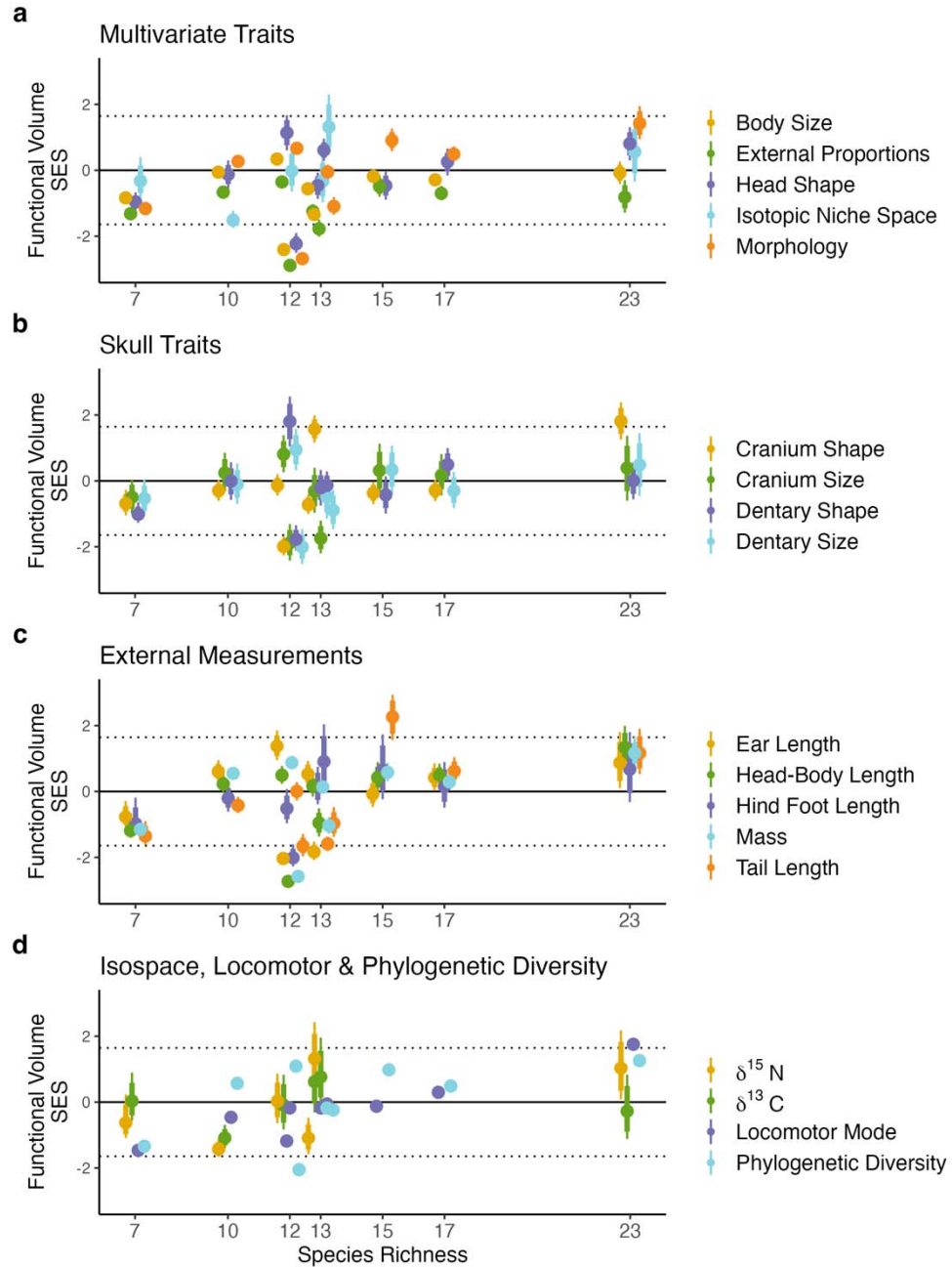
429 density values differed from the volume and density of SES. To avoid the confounding influence
430 of species richness in volume and density estimates we report and discuss only the SES values
431 (Swenson 2014).

432

433 *Effects of Species Richness on Functional Space Volume and Density-* Functional space volume
434 was positively correlated with species richness in seven of the 12 traits (locomotor mode, tail
435 length, head-body length, cranium shape, mass, $\delta^{15}\text{N}$, and hind foot length), as shown by the
436 positive $\beta_{richness}$ slope values from the Bayesian linear models (Figures 3, Table S3) and the
437 greater variance with higher community richness (Figure 3). The remaining five traits (ear
438 length, cranium size, dentary size, dentary shape, and $\delta^{13}\text{C}$) did not substantially increase in
439 volume with increased species richness. Among the multivariate traits, the SES values of total
440 morphological shape increased substantially with species richness while head shape and isotopic
441 niche space show a moderate probability of increasing with species richness (Figures 3, 4, Table
442 S2, S3).

443

444 Linear regression showed that species richness had little to no effect on functional space
445 density (NN SES values) for 11 of the 12 individual traits and three of five multivariate traits
446 (Figures 3, S4, Table S2), consistent with niche expansion. The exceptions were a positive
447 $\beta_{richness}$ slope (i.e., decreased density with richness) for locomotor mode, total morphological
448 shape, and external proportions, suggesting an extreme overdispersion of morphology and
449 locomotor diversity in the richest communities.



450

451 **Figure 3:** Estimated functional volume SES plotted against species richness: **a)** Multivariate trait volumes, **b)** Skull
 452 traits, **c)** External measurements, and **d)** Isotopic measures, locomotor mode, and phylogenetic diversity. Points
 453 represent the mean SES values and error bars indicate the 89% credible intervals. X-axis tick marks show species
 454 richness for each community. Values equal to zero are consistent with null expectations, positive values indicate
 455 overdispersion, and negative values show underdispersion (trait clustering). Dotted lines depict the 89% interval of
 456 the null distribution. The plot of trait densities is shown in the supporting information (Figure S4).
 457

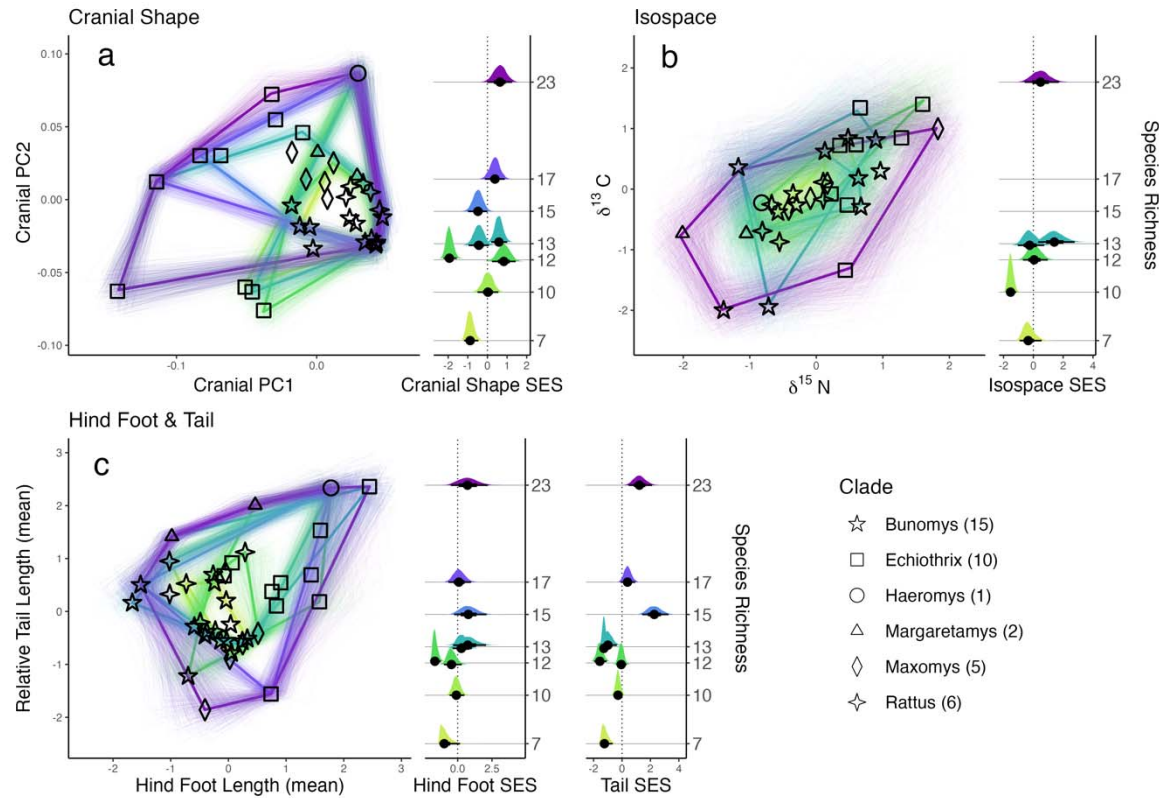
458

459

460 *Phylogenetic Diversity and Functional space-* Phylogenetic diversity (PD) increased with species
461 richness (Figures 3b, 4d, Table S2). Including *Haeromys minahassae* in the estimates of PD
462 changed the PD SES values of the individual communities but had minimal impact on linear
463 regressions (Table S4). Results including *H. minahassae* had a slope ($\beta_{richness}$) of 0.143 (0.03,
464 0.252) while excluding *H. minahassae* generated a slope of 0.169 (89% C.I. of 0.041, 0.295), and
465 we therefore present the results that include *H. minahassae*. Katopasa, a community of 12
466 murines on Sulawesi's Eastern Peninsula, has the lowest PD SES value followed by
467 Bawakaraeng on the Southwestern Peninsula (seven species). Gandang Dewata, the richest
468 community (23 species), has the highest PD SES value (Figure 3a, Table S2). As suspected,
469 functional space volumes vary between clades, though not consistently (Figure S5). For example,
470 the Echiothrix clade has the highest variance in cranial shape, dentary shape, and dentary size but
471 low trait variance for hind-foot length and $\delta^{15}\text{N}$. In contrast, the Maxomys clade has low variance
472 for all trait values except tail length and $\delta^{15}\text{N}$ (Figure S5). This results in different densities of
473 functional space occupation among traits, where some trait volumes, such as cranial space, are
474 strongly influenced by phylogeny, while others, such as isotopic niche space, have high and low
475 values distributed among clades (Figure 4).

476

477



478

479 **Figure 4:** The mode of functional space filling varies among traits. The bivariate plots on the left depict the 2D
480 functional spaces. Each black shape is the mean value of a particular species in each clade (shown in legend). The
481 convex hull colors match the color of the community functional volume SES distributions in the right-hand columns.
482 The thick convex hull lines are mean values, and 500 random samples from the posterior of each trait are shown in
483 thin hull lines. The number of species in each community and each clade used in this study is shown next to the SES
484 distributions in parentheses. All values were scaled to z-scores prior to analyses. **a)** Cranial morphospace values are
485 mostly clustered tightly near the mean of each axis, apart from Echthrix species and the single *Haeromys* species.
486 Intraspecific variance is also relatively low on these axes. **b)** Intraspecific variance is high in isotopic niche space.
487 High and low $\delta^{15}\text{N}$ values are distributed among clades, but that is not the case for $\delta^{13}\text{C}$ values. **c)** Large values of
488 hind foot length belong to members of two clades, while large and small tail length values are dispersed among all
489 six clades, reducing the influence of phylogenetic diversity on tail length disparity.
490

491

492 Discussion

493

494 Variation in species richness among communities of closely related species that inhabit
495 similar environments provides a unique window to explore how interspecific competition may
496 affect community functional richness in the absence of confounding factors like environmental

497 variation (Roughgarden 1976, Swenson et al. 2016). Unfortunately, these species richness
498 anomalies are uncommon (Swenson et al. 2016, Van de Perre et al. 2020). Here we used a large
499 dataset of ecological and morphological traits to estimate the changes in community niche
500 occupancy across a richness gradient on an oceanic island. Though the trait estimates of some
501 species necessarily stem from a small number of specimens, and therefore may be subject to
502 error, our novel probabilistic approach incorporates measurement error and species-level
503 variation into the posterior distribution and propagates this uncertainty through the estimation of
504 community niche space. The functional space of most traits increased with greater species
505 richness among the nine murine communities studied while there was no change in functional
506 space density, consistent with limiting similarity. Locomotor mode disparity has the strongest
507 positive relationship with species richness, but the functional volumes of skull and body shape
508 (indicators of diet, locomotion, and microhabitat use in murines and vertebrates in general;
509 Peters 1986, Losos 2009, Martinez et al. 2018, Nations et al. 2021), also strongly increase with
510 species richness (Figure 2). Measurements of overall body size, cranial size, dentary shape and
511 size, ear length, and $\delta^{13}\text{C}$ values all demonstrate either a weak signal of niche packing, or no
512 signal across the species richness gradient. While the volume of many functional spaces
513 increases with richness, functional space density shows little correlation with species richness for
514 most traits, and it surprisingly decreases with increased richness for external morphology and
515 locomotor mode. These results, along with a general underdispersion of trait values in low-
516 richness communities and overdispersion in high-richness communities (Table S2, Figures 4 &
517 S4), suggest that species in rich communities mitigate competitive interactions by occupying
518 underused niche space. We also found that increasing phylogenetic diversity is a means of
519 increasing functional space occupation. Combined, these results point to species interactions as a

520 mechanism for both phenotypic and phylogenetic overdispersion (Webb et al. 2002, Cavender-
521 Bares et al. 2004, Li et al. 2017) and suggest that, given adequate resources, structural
522 complexity, and evolutionary time, lineages can evolve to occupy unique regions of ecospace,
523 often far from the average trait value, which minimizes niche overlap and cultivates exceptional
524 richness.

525

526 Whether in a single desert valley (Brown 1975), or across continental (Maestri &
527 Patterson 2016, Kohli et al. 2022) and global latitudinal gradients (Karr & James 1975, Pellissier
528 et al. 2018), structurally complex habitats are thought to foster higher species diversity. High
529 plant diversity creates a more complex, vertically structured habitat matrix for other plant and
530 animal species to occupy and has long been tied to higher animal richness (Hutchinson 1959,
531 MacArthur & MacArthur 1961, Scheffers et al. 2013, Oliveira & Scheffers 2019). Our estimates
532 of locomotor-mode occupancy clearly demonstrate that vertical habitat partitioning is critical to
533 maintaining high species richness in Sulawesi murines (Figure 2, Table S2). Strikingly, the
534 density of locomotor trait space decreases along the richness gradient, indicating a very high
535 level of trait overdispersion (Figures 3c & S4). Arboreal, Terrestrial, and Amphibious locomotor
536 modes each provide access to different microhabitats that contain similar resources. Among the
537 23 species found on Mt. Gandang Dewata, the amphibious *Waiomys mamasae*, the terrestrial
538 *Paucidontomys vermidax*, and the arboreal *Sommeromys macrorhinos*, all consume invertebrates
539 and have similar $\delta^{15}\text{N}$ values, yet they are unlikely to compete for resources due to their distinct
540 microhabitat use, a pattern observed in other insular communities of closely related vertebrates
541 (e.g., Jamaican *Anolis*; Shoener 1974). It's worth noting that when the lone amphibious species
542 *Waiomys mamasae*, only known from Gandang Dewata, is removed from the data, the locomotor

543 variance of Gandang Dewata remains the highest among the communities. Morphological
544 measurements are often used to infer locomotor mode in a variety of eco-evolutionary contexts
545 (Ricklefs & Travis 1980, Samuels and Van Valkenburgh 2009, Pianka et al. 2017, Verde-
546 Arregoitia et al. 2019), and our estimates of tail-length variance, a trait correlated with
547 locomotion in murines (Nations et al. 2021), increases with richness at nearly the same rate as
548 locomotor mode (Figure 2). Importantly, our results suggest that locomotor mode rankings may
549 be an effective way to estimate community locomotor variance where continuous trait data are
550 lacking.

551

552 Combining many traits into one multivariate measure of functional diversity is a common
553 approach in evolutionary ecology. Ordination techniques were especially promoted to overcome
554 pitfalls from early community ecology studies that used few, largely subjective measures of
555 resource use (Ricklefs & Travis 1980). However, merging traits into multivariate axes masks
556 trait-specific processes related to functional space (Spasojevic & Suding 2012, Astor et al. 2014).
557 Indeed, our trait volume and density estimates reveal distinct patterns between individual and
558 combined traits. For example, isotopic niche space, a combined signal of $\delta^{15}\text{N}$ and $\delta^{13}\text{C}$ values
559 commonly used in terrestrial ecological studies, exhibits an equivocal signal (Figure 2b), but
560 individual isotopic values reveal that the packing signal originates from the static $\delta^{13}\text{C}$ value
561 along the species richness gradient. The $\delta^{15}\text{N}$ value, a signal of trophic level, expands along the
562 richness gradient, a result that would be overlooked in multivariate analyses. In contrast to $\delta^{15}\text{N}$,
563 dentary shape exhibits an equivocal signal, despite its presumed relationship to dietary niche
564 (Maestri et al. 2016, Kohli et al. 2019). These opposing patterns are only illuminated by
565 analyzing individual traits (Spasojevic & Suding 2012). If we performed this study using only

566 cranial size and dentary shape, which are thought to capture the important axes of size and diet in
567 murine rodents (Rowsey et al. 2019, 2020) and mammals in general (Prevosti et al. 2012,
568 Grossnickle 2020), our results would suggest that functional volume does not increase with
569 species richness.

570

571 The disparity of traits within a clade mediates the impact of phylogenetic diversity on
572 community functional space volume. If trait values are phylogenetically clustered, then
573 increasing phylogenetic diversity is necessary for community niche expansion to occur. But if
574 trait values are phylogenetically overdispersed, niche packing, expansion, or, as we found, both
575 could result from increased phylogenetic diversity. The distribution of traits among clades is of
576 particular interest in communities that are assembled through a mix of colonization and in situ
577 speciation, such as Sulawesi murines, Caribbean anoles, or Hawaiian spiders (Gillespie 2004,
578 Losos 2009, Rowe et al. 2019). Niche divergence has been hypothesized to overcome niche
579 conservatism in communities with an extended history of coevolution, such as those on oceanic
580 islands, likely diminishing the signal of phylogenetic trait clustering (Losos et al. 2003). We find
581 that niche divergence and conservatism may occur simultaneously on different functional traits.
582 For example, the elongate, highly distinct skulls of some species in the Echiothrix clade, the
583 descendants of the first murine colonists on Sulawesi, set them apart from other clades in skull
584 shape and, despite their relatively low abundance, these species overcontribute to community
585 cranial and dentary shape volumes (Figures 3b, 4b, S5). Unlike cranial shape however, the
586 Echiothrix clade occupies a very constrained portion of $\delta^{15}\text{N}$ trophic space. Additionally, trophic
587 level estimates from $\delta^{15}\text{N}$ values are notably dispersed among clades (Figures 4c, S5), and high

588 phylogenetic diversity is not necessary for high isotopic niche space estimates. Are there innate
589 differences in these traits that could lead to opposing patterns of niche conservatism?

590

591 The evolutionary lability of ecologically important traits determines the rate of
592 convergence and divergence possible within a given time frame and can directly influence
593 dispersion of trait values among species (Cavender-Bares et al. 2004). The traits with the highest
594 within-clade variance — $\delta^{15}\text{N}$, tail length, body size — are all thought to be evolutionarily labile.
595 Changes in tail length, body size, and intestinal tract morphology can occur on brief evolutionary
596 time scales (Powell & King 1997, Naya et al. 2008, Kingsley et al. 2017, 2021), whereas
597 morphological changes in cranial shape, such as substantial rostral elongation and the reduction
598 of molar grinding area, may take much longer. Indeed, insular species are known to have rapidly
599 expanded breadths of diet and labile morphological traits following colonization (Stuart et al.
600 2014) and subsequent speciation (Wilson 1959, 1961, Lister 1976, Millien 2006, Rowe et al.
601 2016a). But the extreme cranial morphologies of some Sulawesi murines, particularly those of
602 the oldest radiation on the island (Echiothrix clade), are likely the result of a long process of in-
603 situ evolution (Rowe et al. 2019). In other words, on shorter time scales, similarities in some
604 slowly evolving traits may lead to higher divergences in more labile traits, as evidenced in the
605 Maxomys and Bunomys clades (Figure S5). The opposite pattern may also occur, but only
606 following sufficient evolutionary time. We propose that the evolutionary lability of traits is a
607 determinant of trait value dispersion (Webb et al. 2002, Cavender-Bares et al. 2004), which
608 directly relates to our inferences of functional space occupancy in Sulawesi murine communities.
609 The theory of niche complementarity suggests that a pair of coexisting species that are similar in
610 one trait should diverge in another trait (Schoener 1974). Yet, in an isolated setting, the lability

611 of the traits in question necessarily determines the degree of complementarity possible within a
612 given time frame. Linking trait lability with niche complementarity in an island system has
613 important implications for the generation of functional and taxonomic diversity and may further
614 illuminate the process of niche filling in insular, adaptive radiations.

615

616 Conclusion

617

618 Here we provide evidence that limiting similarity in functional traits reflecting
619 locomotion and microhabitat use plays an important role in the assembly of discrete, montane
620 small mammal communities on an oceanic island. Our results contrast with recent studies that
621 recovered niche packing as key to increased species richness in continental tropical vertebrate
622 communities (Pigot et al. 2016, Peixoto et al. 201, Pellissier et al. 2018, Van de Perre 2020,
623 Dehling et al. 2022, Hughes et al. 2022). Furthermore, our results counter the predictions that
624 niche packing is expected to occur if resources remain constant among communities
625 (Roughgarden 1976). Yet, Roughgarden (1976) posited that the predicted relationship between
626 species richness and resources may be different on remote islands, as the distance from source
627 populations may affect both community richness and the functional trait values of the species
628 present. The organization of distinct montane communities on an oceanic island may be just such
629 an example. The regional murine species pool of Sulawesi is itself structured by idiosyncratic
630 immigration, diversification, and (presumably) extinction dynamics, and the resultant species'
631 functional traits. The species in these communities that occupy the edges of some functional
632 spaces, such as cranial shape (Figure 4), represent morphologies and ecologies found only on
633 Sulawesi or other large, oceanic islands. And the “imperfect isolation” (sensu Samonds et al

634 2013) of Sulawesi allows for other regional murine taxa, often represented by more “average”
635 murine phenotypes, to periodically colonize the island, adding more species into the center of
636 functional space (Figure 4). The presence of such disparate phenotypes and ecologies on
637 Sulawesi (Esselstyn et al. 2012, 2015, Rowe et al. 2014) produces a larger functional space
638 reserve than is available in most, if any, continental rodent systems, nurturing both niche
639 expansion and high species richness. Therefore, the complex topography, isolation, abundant
640 resources, and sequential colonization of Sulawesi might lead to species assembly processes that
641 are typical of other large, oceanic islands, but are atypical of continental systems, “sky islands”,
642 geologically younger islands, or regions with less abundant resources (deserts, high latitude
643 habitats), but the presence of this general pattern remains untested.

644

645

646

647

648

649 **Literature Cited**

650

651 Achmadi, A. S., K. C. Rowe, and J. A. Esselstyn. 2014. New records of two rarely encountered,
652 endemic rats (Rodentia: Muridae: Murinae) from Gunung Gandangdewata, West
653 Sulawesi province. *Treubia* 41:51-60.

654 Adams, D. C., M. Collyer, and A. Kaliontzopoulou. 2021. Geomorph: Software for geometric
655 morphometric analyses. R package version 4.0.3.

656 Astor, T., J. Strengbom, M. P. Berg, L. Lenoir, B. Marteinsdóttir, and J. Bengtsson. 2014.
657 Underdispersion and overdispersion of traits in terrestrial snail communities on islands.
658 *Ecology and Evolution* 4:2090-2102.

659 Baken, E. K., M. L. Collyer, A. Kaliontzopoulou, and D. C. Adams. 2021. Geomorph v4.0 and
660 gmShiny: enhanced analytics and a new graphical interface for a comprehensive
661 morphometric experience. *Methods in Ecology and Evolution*. 12:2355-2363.

662 Baltensperger, A. P., F. Huettmann, J. C. Hagelin, and J. M. Welker. 2015. Quantifying trophic
663 niche spaces of small mammals using stable isotopes ($\delta^{15}\text{N}$ and $\delta^{13}\text{C}$) at two scales across
664 Alaska. *Canadian Journal of Zoology* 93:579-588.

665 Ben-David, M., and E. A. Flaherty. 2012. Stable isotopes in mammalian research: a beginner's
666 guide. *Journal of Mammalogy* 93:312-328.

667 Brown, J. H., and G. A. Lieberman. 1973. Resource utilization and coexistence of seed-eating
668 desert rodents in sand dune habitats. *Ecology* 54:788-797.

669 Brown, J. H. 1975. Geographical Ecology of Desert Rodents. Pages 315-341 in M. L. Cody and
670 J. M. Diamond, editors. *Ecology and Evolution of Communities*. The Belknap Press,
671 Cambridge.

672 Bürkner, P.-C. 2018. Advanced Bayesian Multilevel Modeling with the R Package brms. *The R
673 Journal* 10:395–411.

674 Carlquist, S. 1966. The Biota of Long-Distance Dispersal. I. Principles of Dispersal and
675 Evolution. *The Quarterly Review of Biology* 41: 247–270.

676 Carpenter, B., A. Gelman, M. D. Hoffman, D. Lee, B. Goodrich, M. Betancourt, M. Brubaker, J.
677 Guo, P. Li, and A. Riddell. 2017. Stan: A Probabilistic Programming Language. *Journal
678 of Statistical Software* 76.

679 Cavender-Bares, J., D. D. Ackerly, D. A. Baum, and F. A. Bazzaz. 2004. Phylogenetic
680 Overdispersion in Floridian Oak Communities. *The American Naturalist* 163:823-843.

681 Dehling, D. M., G. V. Dalla Riva, M. C. Hutchinson, and D. B. Stouffer. 2022. Niche packing
682 and local coexistence in a megadiverse guild of frugivorous birds are mediated by fruit
683 dependence and shifts in interaction frequencies. *The American Naturalist* 199:855–868.

684 DeNiro, M. J., and S. Epstein. 1978. Influence of diet on the distribution of carbon isotopes in
685 animals. *Geochimica et Cosmochimica Acta* 42:495-506.

686 DeNiro, M. J., and S. Epstein. 1981. Influence of diet on the distribution of nitrogen isotopes in
687 animals. *Journal of Archeological Science* 45:341-351.

688 Des Roches, S., D. M. Post, N. E. Turley, J. K. Bailey, A. P. Hendry, M. T. Kinnison, J. A.
689 Schweitzer, and E. P. Palkovacs. 2018. The ecological importance of intraspecific
690 variation. *Nature Ecology & Evolution* 2:57-64.

691 Diamond, J. M. 1975. Assembly of Species Communities. Pages 342-444 in M. L. Cody and J.
692 M. Diamond, editors. *Ecology and Evolution of Communities*. The Belknap Press,
693 Cambridge.

694 Dorey, J. B., S. V. Groom, E. H. Freedman, C. S. Matthews, O. K. Davies, E. J. Deans, C.
695 Rebola, M. I. Stevens, M. S. Lee, and M. P. Schwarz. 2020. Radiation of tropical island
696 bees and the role of phylogenetic niche conservatism as an important driver of
697 biodiversity. *Proceedings of the Royal Society B* 287:20200045.

698 Esselstyn, J. A., A. S. Achmadi, and K. C. Rowe. 2012. Evolutionary novelty in a rat with no
699 molars. *Biology Letters* 8:990-993.

700 EsSELSTYN, J. A., A. S. Achmadi, H. Handika, and K. C. Rowe. 2015. A hog-nosed shrew rat
701 (Rodentia: Muridae) from Sulawesi Island, Indonesia. *Journal of Mammalogy* 96:895-
702 907.

703 EsSELSTYN, J. A., A. S. Achmadi, H. Handika, M. T. Swanson, T. C. Giarla, and K. C. Rowe.
704 2021. Fourteen New, Endemic Species of Shrew (Genus *Crocidura*) from Sulawesi
705 Reveal a Spectacular Island Radiation. *Bulletin of the American Museum of Natural
706 History* 454:1-108.

707 FAITH, D. P. 1996. Conservation priorities and phylogenetic pattern. *Conservation Biology*
708 10:1286-1289.

709 FRY, B. 2006. Stable isotope ecology. Springer, New York.

710 GALETTI, M., R. R. RODARTE, C. L. NEVES, M. MOREIRA, and R. COSTA-PEREIRA. 2016. Trophic Niche
711 Differentiation in Rodents and Marsupials Revealed by Stable Isotopes. *PLOS One*
712 11:e0152494.

713 GELMAN A, HILL J. 2006. Data Analysis Using Regression and Multilevel/Hierarchical Models.
714 Cambridge: Cambridge University Press.

715 GELMAN, A., B. GOODRICH, J. GABRY, and A. VEHTARI. 2019. R-squared for Bayesian regression
716 models. *The American Statistician* 73:307-309.

717 GILLESPIE, R. 2004. Community assembly through adaptive radiation in Hawaiian spiders.
718 *Science* 303:356-359.

719 GOTELLI, N. J. 2001. Research frontiers in null model analysis. *Global Ecology and Biogeography*
720 10:337-343.

721 GROSSNICKLE, D. M. 2020. Feeding ecology has a stronger evolutionary influence on functional
722 morphology than on body mass in mammals. *Evolution* 74:610-628.

723 Guillerme T. 2018. *dispRity*: A modular R package for measuring disparity. *Methods in Ecology*
724 and *Evolution* 9:1755-1763.

725 Guillerme, T., M. N. Puttick, A. E. Marcy, and V. Weisbecker. 2020. Shifting spaces: Which
726 disparity or dissimilarity measurement best summarize occupancy in multidimensional
727 spaces? *Ecology and Evolution* 10:7261-7275.

728 Hall, R. 2013. The palaeogeography of Sundaland and Wallacea since the Late Jurassic. *Journal*
729 of *Limnology* 72(s2):1-17.

730 Handika, H., A. S. Achmadi, J. A. Esselstyn, and K. C. Rowe. 2021. Molecular and
731 morphological systematics of the *Bunomys* division (Rodentia: Muridae), an endemic
732 radiation on Sulawesi. *Zoologica Scripta* 50:141-154.

733 Heaney, L. R. 2001. Small mammal diversity along elevational gradients in the Philippines: an
734 assessment of patterns and hypotheses. *Global Ecology and Biogeography* 10:15–39.

735 Hiller, A. E., M. S. Koo, K. R. Goodman, K. L. Shaw, P. M. O’Grady, and R. G. Gillespie. 2019.
736 Niche conservatism predominates in adaptive radiation: comparing the diversification of
737 Hawaiian arthropods using ecological niche modelling. *Biological Journal of the Linnean*
738 *Society* 127:479-492.

739 Hughes, E. C., D. P. Edwards, J. A. Bright, E. J. Capp, C. R. Cooney, Z. K. Varley, and G. H.
740 Thomas. 2022. Global biogeographic patterns of avian morphological diversity. *Ecology*
741 *Letters* 25:598-610.

742 Hutchinson, G. E. 1957. Concluding remarks. *Cold Spring Harbor Symposia on Quantitative*
743 *Biology* 22:415-427.

744 Hutchinson, G. E. 1959. Homage to Santa Rosalia or Why Are There So Many Kinds of
745 Animals? *The American Naturalist* 93:145-159.

746 Imhoff, M. L., L. Bounoua, T. Ricketts, C. Loucks, R. Harriss, and W. T. Lawrence. 2004.

747 Global patterns in human consumption of net primary production. *Nature* 429:870-873.

748 Karr, J. R., and F. C. James. 1975. Ecomorphological Configurations and Convergent Evolution.

749 Pages 258-291 in M. L. Cody and J. M. Diamond, editors. *Ecology and Evolution of*

750 *Communities*. The Belknap Press, Cambridge.

751 Kay, M. 2020. Tidybayes: Tidy data and geoms for Bayesian models. R package version 2.1.1.

752 Kembel, S. W., P. D. Cowan, W. K. Helmus, W. K. Cornwell, H. Morlon, D. D. Ackerly, S. P.

753 Blomberg, and C. O. Webb. 2010. Picante: R tools for integrating phylogenies and

754 ecology. *Bioinformatics* 26:1463-1464.

755 Kingsley, E. P., K. M. Kozak, S. P. Pfeifer, D. S. Yang, and H. E. Hoekstra. 2017. The ultimate

756 and proximate mechanisms driving the evolution of long tails in forest deer mice.

757 *Evolution* 71:261-273.

758 Kingsley, E. P., E. R. Hager, J.-M. Lassance, K. M. Turner, O. S. Harringmeyer, C. Kirby, B. I.

759 Neugeboren, and H. E. Hoekstra. 2024. Adaptive tail-length evolution in deer mice is

760 associated with differential *Hoxd13* expression in early development. *Nature Ecology &*

761 *Evolution*:1–15.

762 Kohli, B. A., and M. A. Jarzyna. 2021. Pitfalls of ignoring trait resolution when drawing

763 conclusions about ecological processes. *Global Ecology and Biogeography* 30:1139–

764 1152.

765 Kohli, B. A., M. J. Miyajima, and M. A. Jarzyna. 2022. Elevational diversity patterns of rodents

766 differ between wet and arid mountains. *Global Ecology and Biogeography* 31:1726-1740.

767 Kohli, B. A., and R. J. Rowe. 2019. Beyond guilds: the promise of continuous traits for

768 mammalian functional diversity. *Journal of Mammalogy* 100:285-298.

769 Kohli, B. A., R. D. Stevens, E. A. Rickart, and R. J. Rowe. 2021. Mammals on mountainsides
770 revisited: Trait-based tests of assembly reveal the importance of abiotic filters. *Journal*
771 *of Biogeography* 48:1606-1621.

772 Kruschke, J. K. 2013. Bayesian estimation supersedes the t test. *Journal of Experimental*
773 *Psychology: General* 142:573.

774 Latham, R. E., and R. E. Ricklefs. 1993. Global Patterns of Tree Species Richness in Moist
775 Forests: Energy-Diversity Theory Does Not Account for Variation in Species Richness.
776 *Oikos* 67:325–333.

777 Lebrun, R. 2018. MorphoDig, an open-source 3D freeware dedicated to biology. IPC5, Paris,
778 France.

779 Legendre, P., and L. Legendre. 2012. Numerical ecology. Elsevier, Amsterdam.

780 Li, Y., B. Shipley, J. N. Price, V. de L. Dantas, R. Tamme, M. Westoby, A. Siefert, B. S.
781 Schamp, M. J. Spasojevic, V. Jung, D. C. Laughlin, S. J. Richardson, Y. L. Bagousse-
782 Pinguet, C. Schöb, A. Gazol, H. C. Prentice, N. Gross, J. Overton, M. V. Cianciaruso, F.
783 Louault, C. Kamiyama, T. Nakashizuka, K. Hikosaka, T. Sasaki, M. Katabuchi, C.
784 Frenette Dussault, S. Gaucherand, N. Chen, M. Vandewalle, and M. A. Batalha. 2018.
785 Habitat filtering determines the functional niche occupancy of plant communities
786 worldwide. *Journal of Ecology* 106:1001–1009.

787 Lister, B. C. 1976. The nature of niche expansion in West Indian *Anolis* lizards I: ecological
788 consequences of reduced competition. *Evolution* 30:659-676.

789 Losos, J. B. 2009. Lizards in an evolutionary tree: ecology and adaptive radiation of anoles.
790 University of California Press, Berkeley.

791 Losos, J. B., M. Leal, R. E. Glor, and K. D. Queiroz. 2003. Niche lability in the evolution of a
792 Caribbean lizard community. *Nature* 424:542–545.

793 Losos, J. B., and R. E. Ricklefs. 2009. Adaptation and diversification on islands. *Nature*
794 457:830-836.

795 M'Closkey, R. T. 1978. Niche separation and assembly in four species of Sonoran Desert
796 rodents. *The American Naturalist* 112:683-694.

797 MacArthur, R. H. 1965. Patterns of species diversity. *Biological Reviews* 40:510–533.

798 MacArthur, R. H. 1970. Species packing and competitive equilibrium for many species.
799 *Theoretical Population Biology* 1:1-11.

800 MacArthur, R., and R. Levins. 1967. The limiting similarity, convergence, and divergence of
801 coexisting species. *The American Naturalist* 101:377-385.

802 MacArthur, R. H., and J. W. MacArthur. 1961. On bird species diversity. *Ecology* 42:594-598.

803 Maestri, R., B. Patterson, R. Fornel, L. Monteiro, and T. De Freitas. 2016. Diet, bite force and
804 skull morphology in the generalist rodent morphotype. *Journal of Evolutionary Biology*
805 29:2191-2204.

806 Maestri, R., and B. D. Patterson. 2016. Patterns of species richness and turnover for the South
807 American rodent fauna. *PLoS One* 11:e0151895.

808 Martinez, Q., R. Lebrun, A. S. Achmadi, J. A. Esselstyn, A. R. Evans, L. R. Heaney, R. P.
809 Miguez, K. C. Rowe, and P.-H. Fabre. 2018. Convergent evolution of an extreme dietary
810 specialization, the olfactory system of worm-eating rodents. *Scientific Reports* 8:17806.

811 May, R. M., and R. H. Mac Arthur. 1972. Niche overlap as a function of environmental
812 variability. *Proceedings of the National Academy of Sciences* 69:1109-1113.

813 McElreath R. 2020 *Statistical Rethinking v2*. Taylor & Francis Group, Boca Raton.

814 Millien, V. 2006. Morphological Evolution Is Accelerated among Island Mammals. *PLOS*
815 *Biology* 4:e321.

816 Musser, G. G. 2014. A systematic review of Sulawesi Bunomys (Muridae, Murinae) with the
817 description of two new species. *Bulletin of the American Museum of Natural History*
818 392.

819 Nations, J. A., L. R. Heaney, T. C. Demos, A. S. Achmadi, K. C. Rowe, and J. A. Esselstyn.
820 2019. A simple skeletal measurement effectively predicts climbing behavior in a diverse
821 clade of small mammals. *Biological Journal of the Linnean Society* 128:323–336.

822 Nations, J. A., G. G. Mount, S. M. Morere, A. S. Achmadi, K. C. Rowe, and J. A. Esselstyn.
823 2021. Locomotory mode transitions alter phenotypic evolution and lineage diversification
824 in an ecologically rich clade of mammals. *Evolution* 75:376-393.

825 Naya, D. E., F. Bozinovic, and W. H. Karasov. 2008. Latitudinal trends in digestive flexibility:
826 testing the climatic variability hypothesis with data on the intestinal length of rodents.
827 *The American Naturalist* 172:122-134.

828 Newsome, S. D., C. Martinez del Rio, S. Bearhop, and D. L. Phillips. 2007. A niche for isotopic
829 ecology. *Frontiers in Ecology and the Environment* 5:429-436.

830 Nugraha, A. M. S. and Hall, R. 2018. Late cenozoic palaeogeography of Sulawesi, Indonesia.
831 *Palaeogeography, Palaeoclimatology, Palaeoecology* 490: 191–209.

832 Oksanen, J, F. Guillaume Blanchet, M. Friendly, R. Kindt, P. Legendre, D. McGlinn, P. R.
833 Minchin, R. B. O'Hara, G. L. Simpson, P. Solymos, M. Henry, H. Stevens, E. Szoecs and
834 H. Wagner (2019). *Vegan: Community Ecology Package*. R package version 2.5-6.

835 Oliveira, B. F., and B. R. Scheffers. 2019. Vertical stratification influences global patterns of
836 biodiversity. *Ecography* 42:249-249.

837 Oliveira, B. F., J. M. Flenniken, R. P. Guralnick, S. E. Williams, and B. R. Scheffers. 2020.

838 Historical environmental stability drives discordant niche filling dynamics across

839 phylogenetic scales. *Journal of Biogeography* 47:807-816.

840 Peixoto, F. P., P. H. P. Braga, and P. Mendes. 2018. A synthesis of ecological and evolutionary

841 determinants of bat diversity across spatial scales. *BMC ecology* 18:1–14.

842 Pellissier, V., J. Y. Barnagaud, W. D. Kissling, Ç. Şekercioğlu, and J. C. Svenning. 2018. Niche

843 packing and expansion account for species richness–productivity relationships in global

844 bird assemblages. *Global Ecology and Biogeography* 27:604-615.

845 Peters, R. H. 1986. *The Ecological Implications of Body Size*. Cambridge University Press,

846 Cambridge.

847 Pianka, E. R. 1974. Niche overlap and diffuse competition. *Proceedings of the National*

848 *Academy of Sciences* 71:2141-2145.

849 Pianka, E. R., L. J. Vitt, N. Pelegrin, D. B. Fitzgerald, and K. O. Winemiller. 2017. Toward a

850 Periodic Table of Niches, or Exploring the Lizard Niche Hypervolume. *The American*

851 *Naturalist* 190:601-616.

852 Pigot, A. L., C. H. Trisos, and J. A. Tobias. 2016. Functional traits reveal the expansion and

853 packing of ecological niche space underlying an elevational diversity gradient in

854 passerine birds. *Proceedings of the Royal Society B: Biological Sciences* 283:20152013.

855 Pinto, G., D. L. Mahler, L. J. Harmon, and J. B. Losos. 2008. Testing the island effect in

856 adaptive radiation: rates and patterns of morphological diversification in Caribbean and

857 mainland *Anolis* lizards. *Proceedings of the Royal Society B: Biological Sciences*

858 275:2749–2757.

859 Powell, R. A., and C. M. King. 1997. Variation in body size, sexual dimorphism and age-specific
860 survival in stoats, *Mustela erminea* (Mammalia: Carnivora), with fluctuating food
861 supplies. *Biological Journal of the Linnean Society* 62:165-194.

862 Prevosti, F. J., G. F. Turazzini, M. D. Ercoli, and E. Hingst-Zaher. 2012. Mandible shape in
863 marsupial and placental carnivorous mammals: a morphological comparative study using
864 geometric morphometrics. *Zoological Journal of the Linnean Society* 164:836-855.

865 Revell, L. J. 2012. Phytools: an R package for phylogenetic comparative biology (and other
866 things). *Methods in Ecology and Evolution* 3:217-223.

867 Ricklefs, R. E., and J. Travis. 1980. A Morphological Approach to the Study of Avian
868 Community Organization. *The Auk* 97:321-338.

869 Rowe, K. C., A. S. Achmadi, and J. A. Esselstyn. 2014. Convergent evolution of aquatic
870 foraging in a new genus and species (Rodentia: Muridae) from Sulawesi Island,
871 Indonesia. *Zootaxa* 3815:541-564.

872 Rowe K.C., A.S. Achmadi, and J.A. Esselstyn. 2016a. Repeated evolution of carnivory among
873 Indo-Australian rodents. *Evolution* 70:653-665.

874 Rowe, K. C., A. S. Achmadi, and J. A. Esselstyn. 2016b. A new genus and species of
875 omnivorous rodent (Muridae: Murinae) from Sulawesi, nested within a clade of endemic
876 carnivores. *Journal of Mammalogy* 97:978-991.

877 Rowe, K. C., A. S. Achmadi, P. H. Fabre, J. J. Schenk, S. J. Steppan, and J. A. Esselstyn. 2019.
878 Oceanic islands of Wallacea as a source for dispersal and diversification of murine
879 rodents. *Journal of Biogeography* 46:2752-2768.

880 Rowsey, D. M., L. R. Heaney, and S. A. Jansa. 2019. Tempo and mode of mandibular shape and
881 size evolution reveal mixed support for incumbency effects in two clades of
882 island-endemic rodents (Muridae: Murinae). *Evolution* 73:1411-1427.

883 Rowsey, D. M., R. M. Keenan, and S. A. Jansa. 2020. Dietary morphology of two island-
884 endemic murid rodent clades is consistent with persistent, incumbent-imposed
885 competitive interactions. *Proceedings of the Royal Society B* 287:20192746.

886 Roughgarden, J. 1976. Resource partitioning among competing species—a coevolutionary
887 approach. *Theoretical Population Biology* 9:388-424.

888 Samonds, K. E., L. R. Godfrey, J. R. Ali, S. M. Goodman, M. Vences, M. R. Sutherland, M. T.
889 Irwin, and D. W. Krause. 2013. Imperfect Isolation: Factors and Filters Shaping
890 Madagascar's Extant Vertebrate Fauna. *PLOS ONE* 8:e62086.

891 Samuels, J. X. 2009. Cranial morphology and dietary habits of rodents. *Zoological Journal of the
892 Linnean Society* 156:864–888.

893 Samuels, J. X., and B. Van Valkenburgh. 2008. Skeletal indicators of locomotor adaptations in
894 living and extinct rodents. *Journal of Morphology* 269:1387-1411.

895 Scheffers, B. R., B. L. Phillips, W. F. Laurance, N. S. Sodhi, A. Diesmos, and S. E. Williams.
896 2013. Increasing arboreality with altitude: a novel biogeographic dimension. *Proceedings
897 of the Royal Society B* 280:20131581.

898 Schoener, T. W. 1974. Resource Partitioning in Ecological Communities: Research on how
899 similar species divide resources helps reveal the natural regulation of species diversity.
900 *Science* 185:27-39.

901 Sikes, R. S., and Animal Care and Use Committee of the American Society of Mammalogists.

902 2016. 2016 Guidelines of the American Society of Mammalogists for the use of wild

903 mammals in research and education. *Journal of Mammalogy* 97:663–688.

904 Spasojevic, M. J., and K. N. Suding. 2012. Inferring community assembly mechanisms from

905 functional diversity patterns: the importance of multiple assembly processes. *Journal of*

906 *Ecology* 100:652-661.

907 Stroud, J. T., and J. B. Losos. 2016. Ecological Opportunity and Adaptive Radiation. *Annual*

908 *Review of Ecology, Evolution, and Systematics* 47:507-532.

909 Stroud, J. T. 2021. Island species experience higher niche expansion and lower niche

910 conservatism during invasion. *Proceedings of the National Academy of Sciences* 118:

911 e2018949118.

912 Stuart, Y. E., T. S. Campbell, P. a. Hohenlohe, R. G. Reynolds, L. J. Revell, and J. B. Losos.

913 2014. Rapid evolution of a native species following invasion by a congener. *Science*

914 346:463-466.

915 Swenson, N. G. 2014. *Functional and Phylogenetic Ecology* in R. Springer, New York.

916 Swenson, N. G., and M. D. Weiser. 2014. On the packing and filling of functional space in

917 eastern North American tree assemblages. *Ecography* 37:1056–1062.

918 Swenson, N. G., M. D. Weiser, L. Mao, S. Normand, M. Á. Rodríguez, L. Lin, M. Cao, and J.-C.

919 Svenning. 2016. Constancy in functional space across a species richness anomaly. *The*

920 *American Naturalist* 187:E83-E92.

921 Tews, J., Brose, U., Grimm, V., Tielbörger, K., Wichmann, M. C., Schwager, M. and Jeltsch, F.

922 2004. Animal species diversity driven by habitat heterogeneity/diversity: the importance

923 of keystone structures. *Journal of Biogeography* 31: 79–92.

924 Van de Perre, F., M. R. Willig, S. J. Presley, I. J.-C. Mukinzi, M. S. Gambalemoke, H. Leirs, and
925 E. Verheyen. 2020. Functional volumes, niche packing and species richness:
926 biogeographic legacies in the Congo Basin. Royal Society Open Science 7:191582.

927 Vaughan, D, and M. Dancho 2021. furrr: Apply Mapping Functions in Parallel using Futures. R
928 package version 0.2.2.

929 Verde Arregoitia, L. D., D. O. Fisher, and M. Schweizer. 2017. Morphology captures diet and
930 locomotor types in rodents. Royal Society Open Science 4:160957.

931 Violette, C., B. J. Enquist, B. J. McGill, L. Jiang, C. H. Albert, C. Hulshof, V. Jung, and J.
932 Messier. 2012. The return of the variance: intraspecific variability in community ecology.
933 Trends in Ecology & Evolution 27:244-252.

934 Webb, C. O. 2000. Exploring the phylogenetic structure of ecological communities: an example
935 for rain forest trees. The American Naturalist 156:145-155.

936 Webb, C. O., D. D. Ackerly, M. A. McPeek, and M. J. Donoghue. 2002. Phylogenies and
937 community ecology. Annual Review of Ecology and Systematics 33:475-505.

938 Weiher, E., and P. A. Keddy. 1995. Assembly rules, null models, and trait dispersion: new
939 questions from old patterns. Oikos:159-164.

940 Wickham, H., M. Averick, J. Bryan, W. Chang, L. D. A. McGowan, R. François, G. Grolemund,
941 A. Hayes, L. Henry, and J. Hester. 2019. Welcome to the Tidyverse. Journal of Open
942 Source Software 4:1686.

943 Wilson, D. E., R. A. Mittermeier, and T. E. Lacher. 2019. Handbook of the Mammals of the
944 World. Lynx Editions, Barcelona.

945 Wilson, E. O. 1959. Adaptive shift and dispersal in a tropical ant fauna. Evolution 13:122-144.

946 Wilson, E. O. 1961. The Nature of the Taxon Cycle in the Melanesian Ant Fauna. *The American*
947 *Naturalist* 95:169-193.

948 Woodward, G., and A. G. Hildrew. 2002. Body□size determinants of niche overlap and
949 intraguild predation within a complex food web. *Journal of Animal Ecology* 71:1063-
950 1074.

951 Xu, X., D. Dimitrov, N. Shrestha, C. Rahbek, and Z. Wang. 2019. A consistent species richness-
952 climate relationship for oaks across the Northern Hemisphere. *Global Ecology and*
953 *Biogeography* 28:1051–1066.

954

955

956

957

958

959

960

961

962

963

964

965 **References Only Cited in the Online Supplement**

966 Achmadi, A. S. 2010. Taxonomic Status of Spiny Rats (*Maxomys* Jentink, Rodentia) from
967 Indonesia and Malaysia Based on Morphological Study. *Treubia* 37:49-82.

968 Fry, B. 2006. Stable isotope ecology. Springer, New York.

969 Hückstädt, L., J. Burns, P. Koch, B. McDonald, D. E. Crocker, and D. Costa. 2012. Diet of a
970 specialist in a changing environment: the crabeater seal along the western Antarctic
971 Peninsula. *Marine Ecology Progress Series* 455:287-301.

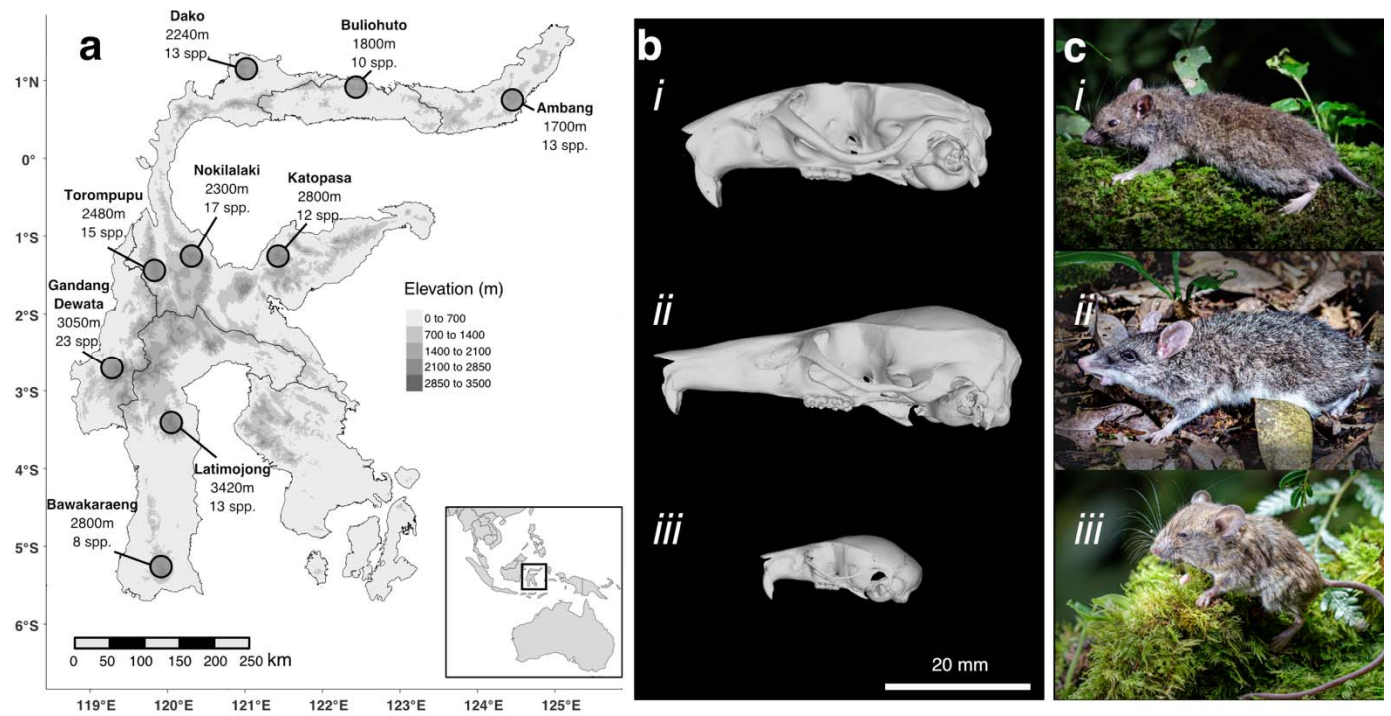
972 Kruschke, J. K. 2013. Bayesian estimation supersedes the t test. *Journal of Experimental
973 Psychology: General* 142:573.

974 McElreath R. 2020 *Statistical Rethinking v2*. Taylor & Francis Group. Boca Raton.

975 Musser, G. G., and M. D. Carleton. 2005. Superfamily Muroidea. Pages 894–1531 in D. E.
976 Wilson, Reeder D.M., editor. *Mammal species of the world: a taxonomic and geographic
977 reference*. Johns Hopkins Univ. Press, Baltimore.

978

979



980

981 **Figure 1:** Small mammal surveys of nine mountains a) on the oceanic island of Sulawesi revealed varying murine
982 rodent species richness across the island. Each mountain on the map is labeled with the maximum elevation and the
983 number of murine rodent species present. All but Latimojong were surveyed within 600m of the summit. b) The
984 diversity of Sulawesi murines is exceptional and includes unique forms that live alongside species with more
985 “typical” ecologies and morphologies, as demonstrated from surfaces of cranial μCT scans of *i – Rattus hoffmanni*, a

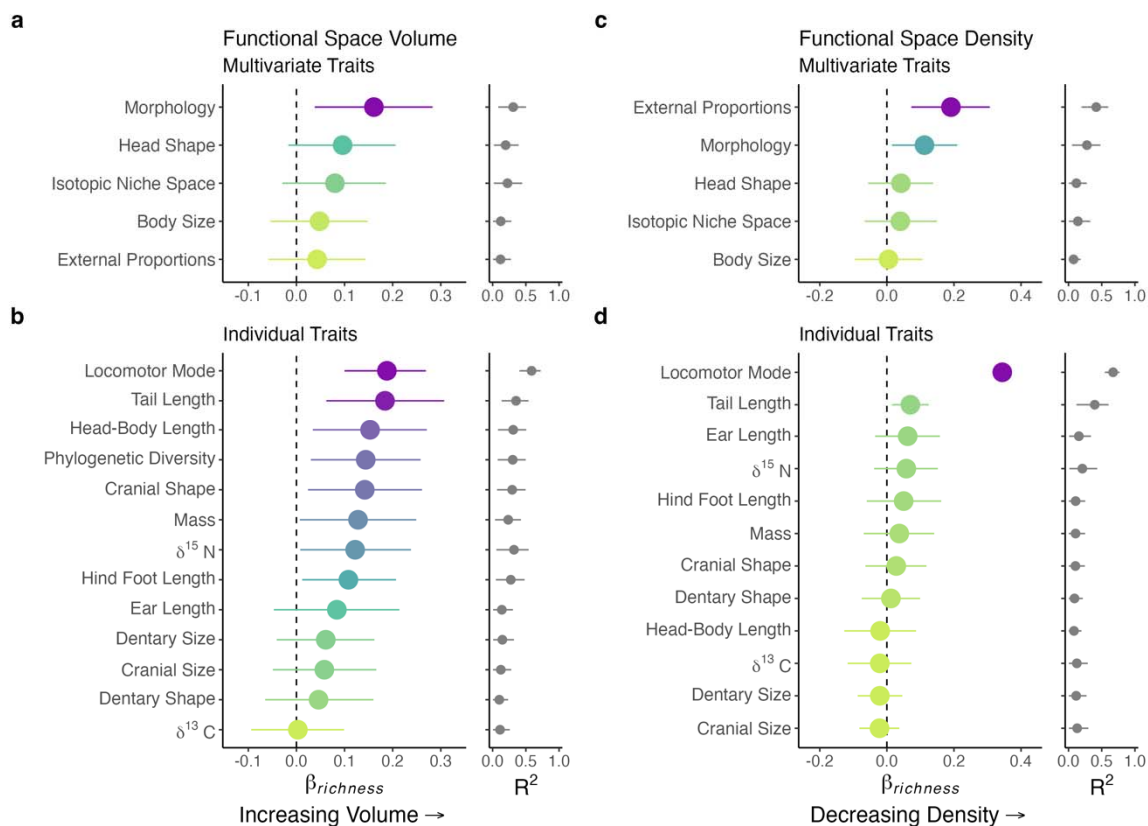
986 “typical” murine morphology and ecology, *ii* – the shrew rat *Echinothrix leucura* with its extremely elongate rostrum
 987 and soft invertebrate diet, *iii* – the arboreal *Haeromys minahassae*, with a short rostrum and very small size. c)
 988 Photographs: *i* – *Rattus hoffmanni*, *ii* – *Echinothrix leucura*, and *iii* – *Haeromys minahassae*.

989
 990
 991

Clade	Crown Age	Species Sampled
Echinothrix	5.11 (4.49-5.69)	10 (10)
Maxomys	3.72 (3.21-4.29)	5 (5)
Bunomys	3.45 (3.09-3.81)	15 (15)
Margaretamys	2.92 (2.29-3.51)	2 (4)
Rattus*	1.57 (1.22-1.95)	6 (6)
Haeromys [†]	Indeterminate	1 (1)

992 **Table 1:** Ages of six clades descended from Sulawesi colonists. Median age in millions of years is reported with
 993 95% credible intervals in parentheses. Species sampled reports the number of species in this study with overall clade
 994 richness in parentheses and demonstrates near complete sampling. The two unsampled *Margaretamys* species were
 995 not detected in the localities in this study. All ages taken from Rowe et al. 2019. *There were likely two
 996 colonizations by the ancestors of native *Rattus* spp., the second of which occurred 1.16-0.6 Ma (Rowe et al. 2019),
 997 however, all *Rattus* in this study form a clade relative to other Sulawesi murines. Two human commensal *Rattus*
 998 spp. found on Sulawesi were excluded. [†]The age of arrival of the *Haeromys* clade is unknown as other species of
 999 *Haeromys* from Borneo have yet to be included in phylogenetic analyses.

1000



1001

1002 **Figure 2:** The effect of species richness on community functional space volume (a, b) and density (c, d). X-axes
 1003 show the $\beta_{richness}$ estimates (the regression slope) for each trait space (y-axis) on the left and the Bayesian R^2 for

1004 each $\beta_{richness}$ estimate on the right. Colored point intervals show 89% probability of $\beta_{richness}$ estimates (effect
1005 size), with color varying by $\beta_{richness}$ value. Black point intervals show 50% posterior estimates of Bayesian R^2 for
1006 each trait space. Density was estimated using the mean nearest neighbor (NN), and a high NN distance indicates low
1007 density. Four of the five multivariate traits (**a**) and seven of the 12 individual traits (**b**), show an increase in
1008 functional space volume (trait variance) with greater richness (i.e., positive $\beta_{richness}$). Phylogenetic diversity also
1009 increases with species richness (**b**). All multivariate traits (**c**) and individual traits (**d**) show a stable or, surprisingly,
1010 decreasing functional space density (increased NN distance) with greater species richness.

1011

1012

1013

1014

1015

1016

1017

1018

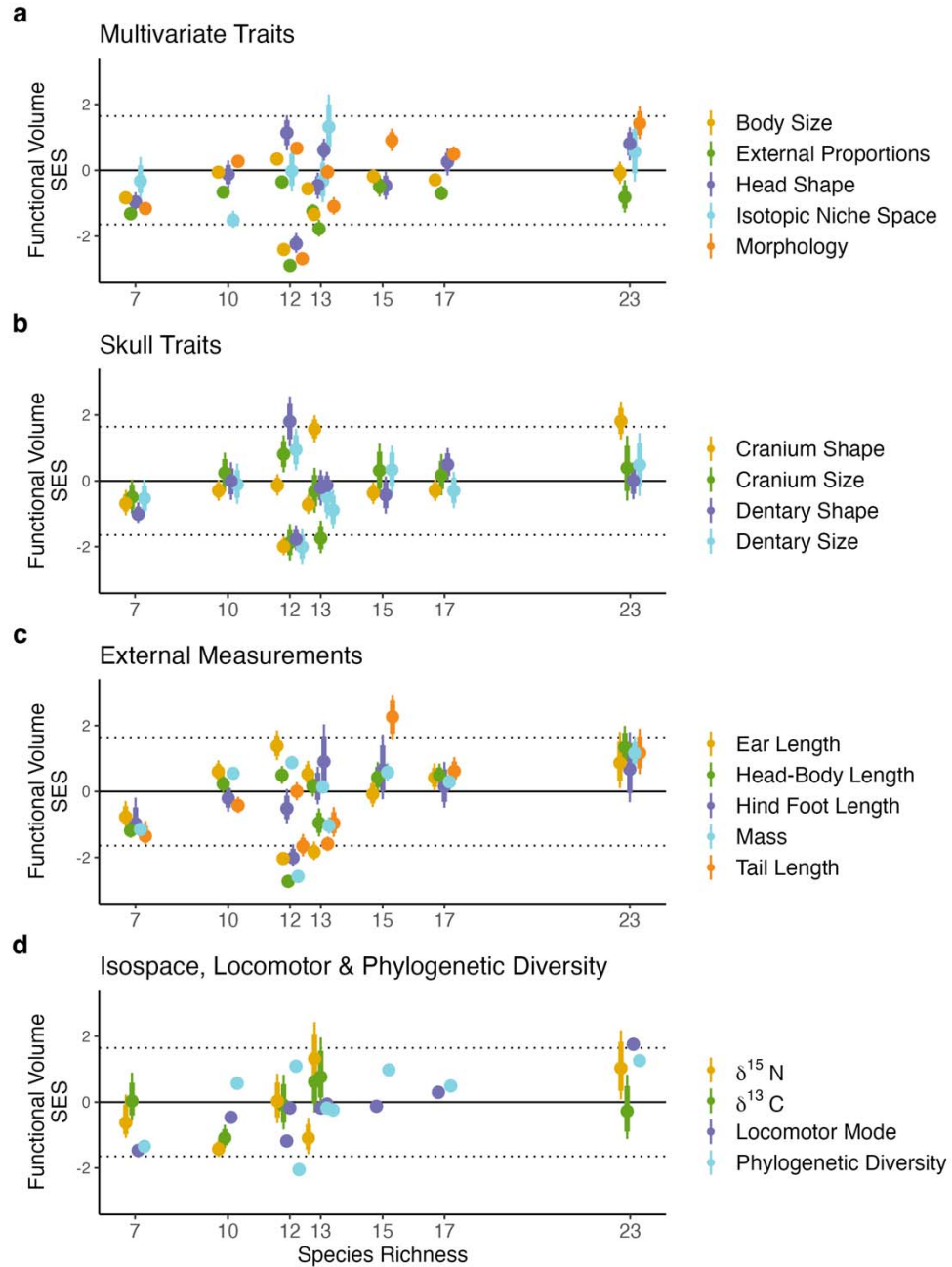
1019

1020

1021

1022

1023



1024

1025 **Figure 3:** Estimated functional volume SES plotted against species richness: **a)** Multivariate trait volumes, **b)** Skull
 1026 traits, **c)** External measurements, and **d)** Isotopic measures, locomotor mode, and phylogenetic diversity. Points
 1027 represent the mean SES values and error bars indicate the 89% credible intervals. X-axis tick marks show species
 1028 richness for each community. Values equal to zero are consistent with null expectations, positive values indicate
 1029 overdispersion, and negative values show underdispersion (trait clustering). Dotted lines depict the 89% interval of
 1030 the null distribution. The plot of trait densities is shown in the supporting information (Figure S4).

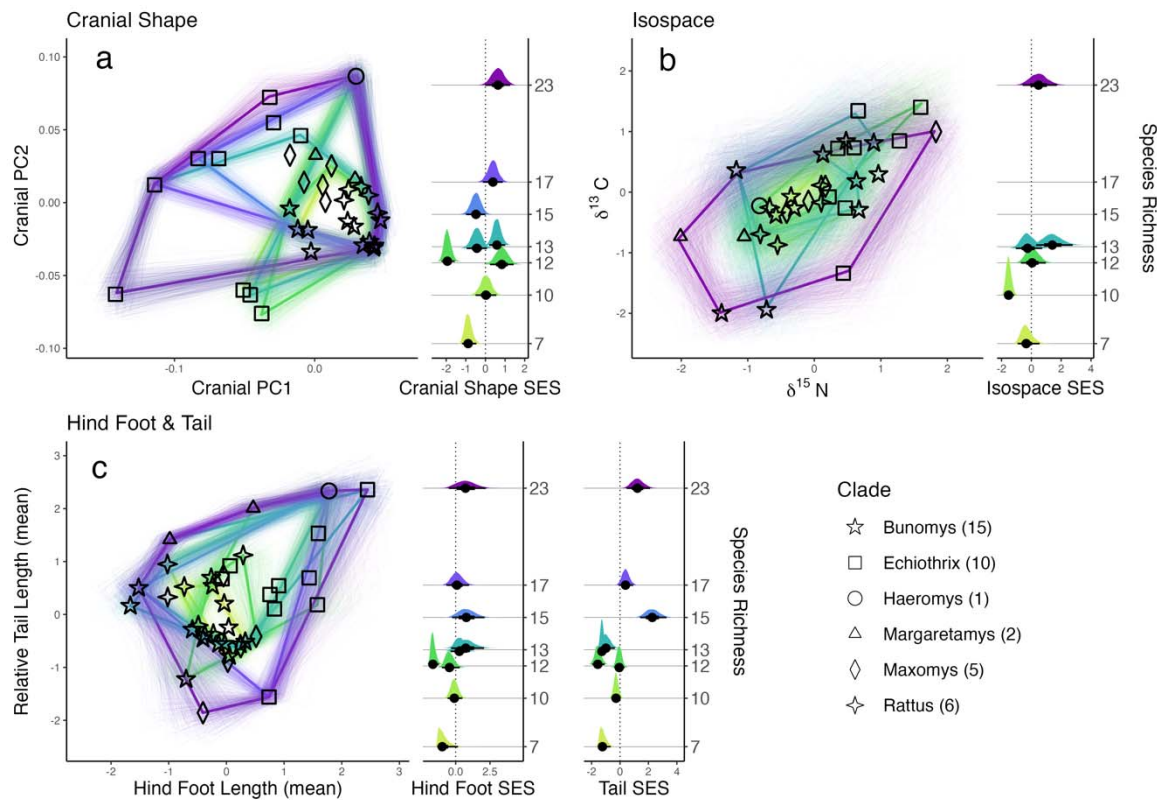
1031

1032

1033

1034

1035



1036

1037 **Figure 4:** The mode of functional space filling varies among traits. The bivariate plots on the left depict the 2D
1038 functional spaces. Each black shape is the mean value of a particular species in each clade (shown in legend). The
1039 convex hull colors match the color of the community functional volume SES distributions in the right-hand columns.
1040 The thick convex hull lines are mean values, and 500 random samples from the posterior of each trait are shown in
1041 thin hull lines. The number of species in each community and each clade used in this study is shown next to the SES
1042 distributions in parentheses. All values were scaled to z-scores prior to analyses. **a**) Cranial morphospace values are
1043 mostly clustered tightly near the mean of each axis, apart from Echiorhix species and the single Haeromys species.
1044 Intraspecific variance is also relatively low on these axes. **b**) Intraspecific variance is high in isotopic niche space.
1045 High and low $\delta^{15}\text{N}$ values are distributed among clades, but that is not the case for $\delta^{13}\text{C}$ values. **c**) Large values of
1046 hind foot length belong to members of two clades, while large and small tail length values are dispersed among all
1047 six clades, reducing the influence of phylogenetic diversity on tail length disparity.

1048

1049